Dielectric Properties of Wood

AUTHOR(S):

NORIMOTO, Misato

Dielectric Properties of Wood

Misato NORIMOTO*

Contents

Introduction

The dielectric behaviors of wood depend markedly on the chemical and fine structures as well as on the macroscopic structure of wood. The investigation on the dielectric properties of wood, therefore, provides an important approach to an understanding of the correlation between the properties and the structure of wood. The purpose of this article is to make clear the mechanism of the dielectric

* Division of Wood Physics.

relaxation processes occurred in wood and wood constituents in the dry state, and moreover to evaluate quantitatively the magnitude of the dielectric constants of wood in the three principal directions.

1. Dielectric relaxations of wood and wood constituents

1.1 Phenomenological theory

Dielectric constant and loss factor

The electric field inside a dielectric is described by the two field quantities, i.e., the electric field strength E and the electric displacement D. If P is the polarization of a dielectric, the correlation among E, D and P is given by $D=E+4\pi P$, and the static dielectric constant ϵ_0 is defined by the ratio D/E. In the case of an altering field, P generally lags behind E by some phase angle δ. If E and D are expressed in a complex form, i.e., $E=E_0\exp(i\omega t)$ and $D=D_0\exp(i\omega t-i\delta)$, where E_0 and D_0 are the field and displacement amplitudes respectively and ω is the angular frequency, then the complex dielectric constant ($\epsilon^*=\epsilon'-i\epsilon''$) is defined by the ratio D*/E*, where ϵ' and ϵ'' are called the dielectric constant and loss factor respectively and they usually depend on both frequency and temperature. The quantities ϵ' and ϵ'' are not independent of each other and the relation between the two quantities is given by[1]

$$\epsilon'(\omega)-\epsilon_\infty=\frac{2}{\pi}\int_0^\infty \epsilon''(x)\frac{x}{x^2-\omega^2}dx, \tag{1.1}$$

$$\epsilon''(\omega)=\frac{2}{\pi}\int_0^\infty \left\{\epsilon'(x)-\epsilon_\infty\right\}\frac{\omega}{\omega^2-x^2}dx, \tag{1.2}$$

where ϵ_∞ is the dielectric constant at frequencies in infra-red region and x is an integration variable. The integrals in these equations are principal values respectively. The heat W produced per unit second and unit volume in a dielectric in an altering field is given by[1]

$$W=\frac{\omega}{2\pi}\left(\frac{1}{4\pi}\int_0^{2\pi/\omega} E\frac{\partial D}{\partial t}dt\right)=\frac{\epsilon''E_0^2\omega}{8\pi}. \tag{1.3}$$

Thus, the quantities ϵ' and ϵ'' represent measures of polarization and energy dissipation in a dielectric respectively.

The phenomenon in which ϵ' decreases with increase of freauency is called the anomalous dispersion. In the dispersion region the ϵ'' curve, i.e., the absorption curve, reaches a maximum. Figs. (1.1) and (1.2) show the plots of ϵ' and ϵ'' for dry HOONOKI (*Magnolia obovata* THUNB.) in the longitudinal direction against logarithmic frequency log f and temperature T respectively. The two quantities depend markedly on both frequency and temperature. Furthermore, they depend on specific gravity as can be seen in Table (1.1) and Fig. (1.3). The value of ϵ'

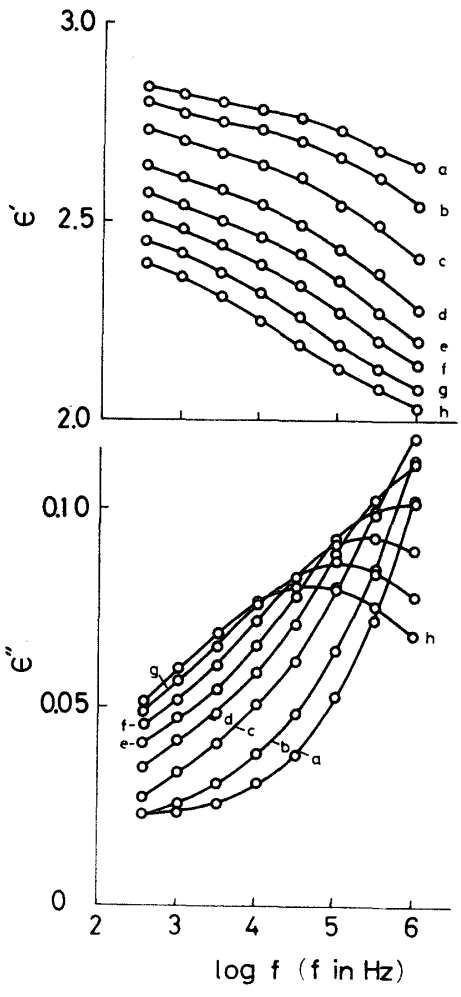

Fig. 1.1. Frequency dependence of ϵ' and ϵ'' at several temperatures for dry HOONOKI in L direction. (m.c.= ca. 0.3%, γ=0.55, a: 53°C b: 36°C c: 15°C d: −0.5°C e: −10°C f: −20°C g: −30°C h: −40.5°C).

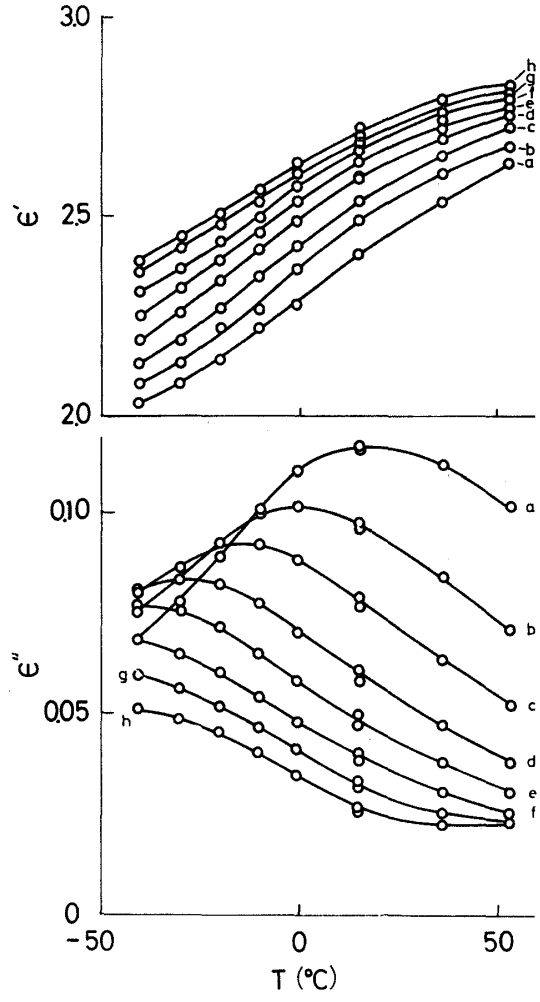

Fig. 1.2. Temperature dependence of ϵ' and ϵ''at several frequencies for dry HOONOKI in L direction. (m.c.= 0.3%, γ=0.55, a: 1MHz b: 300kHz c: 100kHz d: 30kHz e: 10kHz f: 3kHz g: 1kHz h: 330Hz).

of wood decreases generally in the order, L (longitudinal direction)>R (radial direction)≧T (tangential direction).

Thus, the dielectric properties are generally described by ϵ' and ϵ'', in other words by P. The polarization P is associated with displacements of charges induced inside a dielectric by an external field, in which there are two types, i.e., one is the elastic displacement and the other is the displacement to another equilibrium position. The polarization associated with the elastic displacement of charges is termed the deformation polarization P_D, which consists of the optical polarization due to the displacement of electrons and the infra-red polarization due to the displacement of atoms or groups of atoms. On the other hand, another polarization

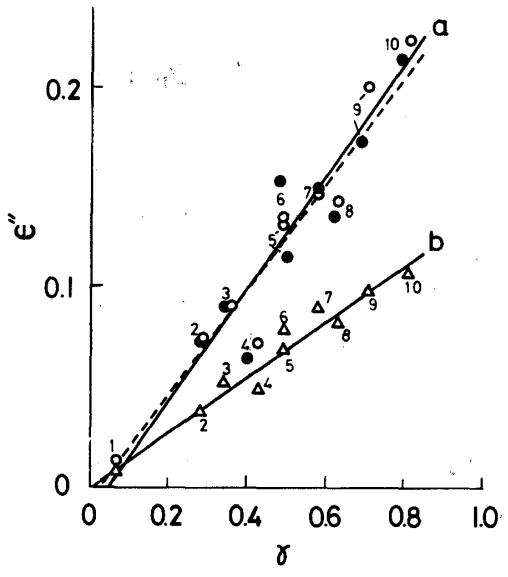

Fig. 1.3. Specific gravity dependence of ϵ'' at 1 MHz for absolutely dried woods in L direction. (open circles and triangles : untreated samples, closed circles : samples treated with the mixture of alcohol and benzene, a : 31°C b : −51°C, 1 : BALSA (*Ochroma* spp.) 2 : KIRI 3 : SUGI (*Cryptomeria japonica* D. DON) 4 : KUSUNOKI (*Cinnamomum camphora* SIEB.) 5 : HOONOKI 6 : HINOKI 7 : AKAMATSU 8 : MAKANBA 9 : KEYAKI (*Zelkowa seerrata* MAKINO) 10 : KASHI). a : $\epsilon''=0.284\gamma-0.015$ (solid line) r=0.967, $\epsilon''=0.268\gamma-0.009$ (dotted line) r=0.947. b : $\epsilon''=0.141\gamma-0.0017$ (solid line) r=0.974.

Table 1.1. Values of dielectric constant at 20°C and 1 MHz for absolutely dried woods.

Species	Specific gravity γ	ϵ'		
		L	R	T
KIRI (*Paulownia tomentosa* STEUD.)	0.25	1.75		
	0.29		1.60	
	0.26			1.51
HINOKI (*Chamaceyparis obtusa* ENDL.)	0.35	2.19		
	0.37		1.77	
	0.40			1.75
	0.53	2.48	1.94	
	0.54			1.88
AKAMATSU (*Pinus densiflora* SIEB. et ZUCC.)	0.46	2.22	1.79	1.77
HOONOKI (*Magnolia obovata* THUNB.)	0.48	2.49	1.91	1.77
MAKANBA (*Betula maximowicziana* REOGEL)	0.61	2.71	2.03	2.01
KASHI (*Quercus* spp.)	0.81	3.08	2.31	2.40

is termed the orientation polarization P_0. When a constant field is suddenly applied to a dielectric substance, the polarization occurs. This polarization process involves instantaneously occurring polarization P_D and gradually occurring polarization P_0. When the applied field is removed after a sufficiently long period of time, P shows first an instantaneous reduction corresponding to P_D followed by an exponential decay $P_0 \exp(-t/\tau)$ with time t. When t has such a value that $t=\tau$, P must have decayed to $P_0 \exp(-1)$. Here, τ is a quantity called the relaxation time. In the case of an altering field the complex dielectric constant of the substance having a single relaxation time is written as

$$\epsilon^* - \epsilon_\infty = \frac{\epsilon_0 - \epsilon_\infty}{1 + i\omega\tau}. \qquad (1.4)$$

Eq. (1.4), however, can not describe strictly the dielectric behavior of substances like wood. Therefore, Eq. (1.4) must be generalized as follows.

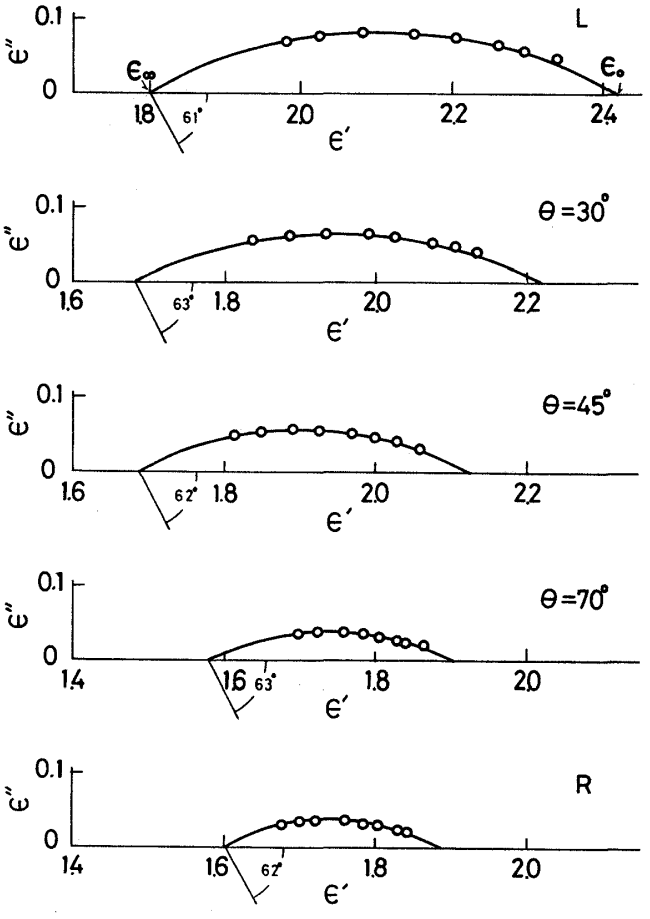

Fig. 1.4. COLE-COLE plot for absolutely dried HOONOKI in LR plane. (θ : grain angle, $\gamma=0.50$, $T=-40°C$).

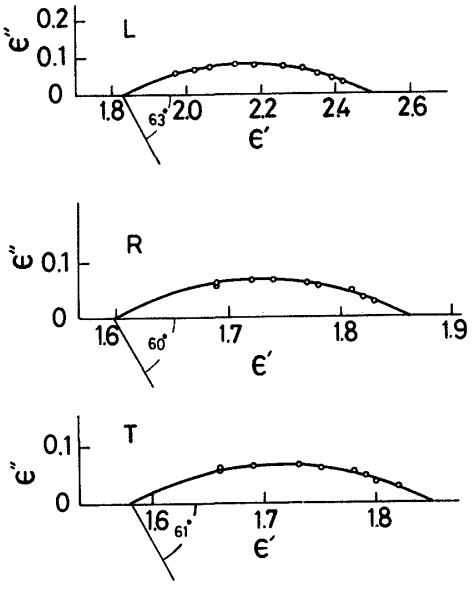

Fig. 1.5. COLE-COLE plot for absolutely dried western hemlock in L, R and T directions. ($\gamma=0.48$, $T=-58°C$).

$$\epsilon^*-\epsilon_\infty=\int_0^\infty \frac{y(\tau)d\tau}{1+i\omega\tau}, \tag{1.5}$$

$$\epsilon_0-\epsilon_\infty=\int_0^\infty y(\tau)d\tau,$$

where the function $y(\tau)$ is called the distribution of relaxation times.

Distribution of relaxation times

Separating Eq.(1.4) into real and imaginary parts,

$$\epsilon'=\epsilon_\infty+\frac{\epsilon_0-\epsilon_\infty}{1+\omega^2\tau^2}, \tag{1.7}$$

$$\epsilon''=\frac{(\epsilon_0-\epsilon_\infty)\omega\tau}{1+\omega^2\tau^2}. \tag{1.8}$$

Combining Eqs. (1.7) and (1.8) to eliminate $\omega\tau$, yiels

$$\left(\epsilon'-\frac{\epsilon_0+\epsilon_\infty}{2}\right)^2+\epsilon''=\left(\frac{\epsilon_0-\epsilon_\infty}{2}\right)^2. \tag{1.9}$$

Eq. (1.9) predicts that the plot of ϵ'' against ϵ' in a complex plane, i.e., the COLE-COLE plot, gives a semicircle of radius $(\epsilon_0-\epsilon_\infty)/2$. However, COLE and coworker have found that these plots for a number of dielectric substances give depressed semicircles. Then, they have modified Eq. (1.4) by replacing the term $(1+i\omega\tau)$ by $1+(i\omega\tau_0)^{1-\alpha}$.

Hence

$$\epsilon^*-\epsilon_\infty=\frac{\epsilon_0-\epsilon_\infty}{1+(i\omega\tau_0)^{1-\alpha}}, \tag{1.10}$$

where τ_0 and $\alpha(0\leqq\alpha\leqq1)$ are the generalized relaxation time and the parameter relating to the distribution of relaxation times respectively. The distribution function $\Phi(s)$ for Eq. (1.10) is given by[2]

$$\Phi(s)=\frac{1}{2\pi}\frac{\sin\alpha\pi}{\cosh(1-\alpha)s-\cos\alpha\pi}, \tag{1.11}$$

$$s=\ln\frac{\tau}{\tau_0},\quad \Phi(s)\equiv\frac{\tau y(\tau)}{\epsilon_0-\epsilon_\infty}.$$

In Figs. (1.4) and (1.5) the COLE-COLE plots for HOONOKI in LR plane[3] and for western hemlock (*Thuja heterophylla* SARGENT) in the three principal directions[4] are shown. The loci in a complex plane show depressed semicircles, so that the relaxation process of wood can be represented by Eq. (1.10). Furthermore, in Table (1.2) the values of $(\epsilon_0-\epsilon_\infty)$ and $(\pi/2)\alpha$ determined from the COLE-COLE plots for four wood species at various temperatures are listed. The value of α increases with decrease of T, indicating that the width of the distribution of relaxation times becomes wider with decreasing T but it appears to be independent of both species and grain directions. On the other hand, the $(\epsilon_0-\epsilon_\infty)$ value which represents the magnitude of relaxation is the highest in L direction and decreases with increase of grain angle if a comparison is made at the same temperature and specific gravity. In Fig. (1.6) $(1-\alpha)$ are plotted against T.

Table 1.2. Values of $(\epsilon_0-\epsilon_\infty)$ and $\frac{\pi}{2}\alpha$ for absolutely dried woods.

Species	γ	D*	T (°C)	$\epsilon_0-\epsilon_\infty$	$\frac{\pi}{2}\alpha$(°)
HOONOKI	0.48	L	3	0.63	52
			−19	0.61	55
			−49	0.63	62
	0.50	L	−40	0.64	61
		θ=30°**		0.56	63
		45		0.45	62
		70		0.33	63
		R		0.28	62
	0.55	L	20	0.79	53
			0	0.76	58
western hemlock	0.48	L	−58	0.66	64
		R		0.26	61
		T		0.27	61
KEYAKI	0.65	L		0.84	63
		T		0.33	66
KASHI	0.81	L		0.83	64
		R		0.37	65
		T		0.32	64

* Direction of measurement
** Grain angle

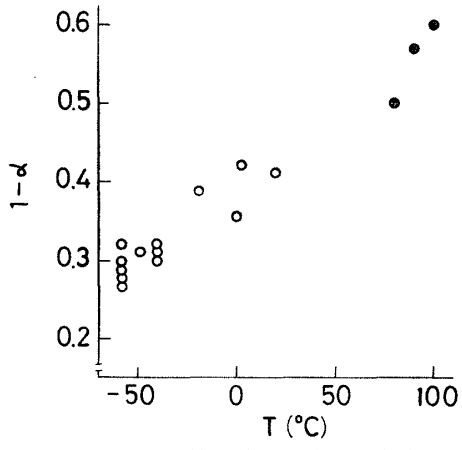

Fig. 1.6. Plot of $(1-\alpha)$ against T for absolutely dried woods. (open circles: see Table 1.2, closed circles After NANNACY[5]).

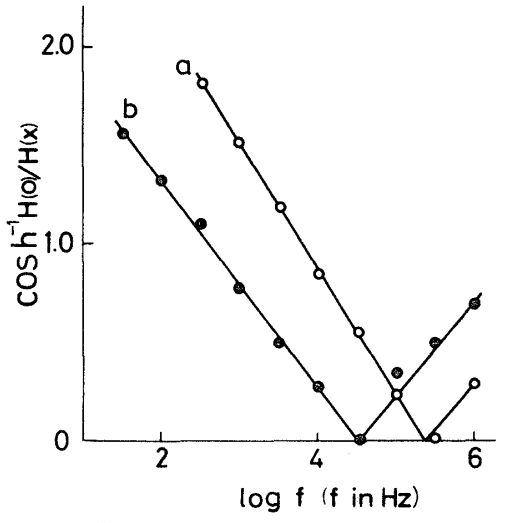

Fig. 1.7 $\text{Cosh}^{-1}H(0)/H(x)$ versus log f curves for absolutely dried HOONOKI in L direction. (a: γ=0.55 T=−20°C, b: γ=0.48 T=−49°C).

FUOSS and KIRKWOOD[6] have reported that $\Phi(s)$ can be calculated strictly from

$$\pi\Phi(s) = H\left(s+\frac{i\pi}{2}\right)+H\left(s-\frac{i\pi}{2}\right), \tag{1.12}$$

$$H(\omega) = \frac{1}{\epsilon_0-\epsilon_\infty}\int_0^\infty \frac{y(\tau)\omega\tau}{1+\omega^2\tau^2}d\tau.$$

If H(x) can be represented by H(0)sech(α'x), where $x=\ln(\omega_0/\omega)$, then $\Phi(s)$ is given by

$$\Phi(s) = \frac{2H(0)}{\pi}\cdot\frac{\cos\left(\frac{\alpha'\pi}{2}\right)\cos h(\alpha's)}{\cos^2\left(\frac{\alpha'\pi}{2}\right)+\sin h^2(\alpha's)}, \tag{1.13}$$

where α' is a parameter relating to the distribution of relaxation times and H(0) is the maximum value of H(x). Here H(0) and $(\epsilon_0-\epsilon_\infty)$ can be calculated from

$$H(0) = \frac{\alpha'}{2}, \quad \epsilon_0-\epsilon_\infty = \frac{2\epsilon''_m}{\alpha'}, \tag{1.14}$$

where ϵ''_m is the maximum value of ϵ''. The plot of $\cosh^{-1}H(0)/H(x)$ against log f for absolutely dried HOONOKI is linear as shown in Fig. (1.7)[4,7]. In Table (1.3) the values of $(\epsilon_0-\epsilon_\infty)$ and α' for absolutely dried HOONOKI are listed[3,4,7]. The $(\epsilon_0-\epsilon_\infty)$ values calculated from the sech law are slightly higher than those from the COLE-COLE law.

Fig. (1.8) shows $\Phi(\ln\tau)$ calculated from Eqs. (1.11) and (1.13), and by the following approximate methods[4,8].

$$\Phi_0(\ln\tau) = \frac{2}{\pi}\frac{\epsilon''}{\epsilon_0-\epsilon_\infty}, \tag{1.15}$$

$$\Phi_1(\ln\tau) = -d\left(\frac{\epsilon'-\epsilon_\infty}{\epsilon_0-\epsilon_\infty}\right)\Big/ d\ln\omega,$$

$$\Phi_2(\ln\tau) = B\frac{\epsilon''}{\epsilon_0-\epsilon_\infty}\left(1-\left|d\log\left(\frac{\epsilon''}{\epsilon_0-\epsilon_\infty}\right)\Big/ d\log\omega\right|\right), \tag{1.16}$$

Table 1.3. Values of $(\epsilon_0-\epsilon_\infty)$ and α' for absolutely dried HOONOKI.

γ	D	T (°C)	α'	$\epsilon_0-\epsilon_\infty$
0.48	L	−49	0.22	0.72
0.55	L		0.22	0.75
	θ=30°		0.20	0.67
0.50	45	−40	0.21	0.55
	75		0.21	0.38
	R		0.23	0.31
0.55	L	−20	0.29	0.64

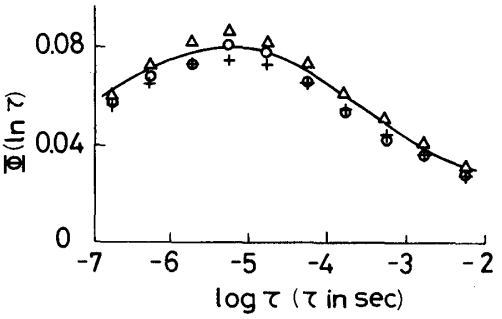

Fig. 1.8. Distribution function of relaxation times at −49°C for absolutely dried HOONOKI in L direction. (γ=0.48, solid line : Eq. (1.15) open circles : Eq. (1.16) triangles : Eq. (1.11) crosses : Eq. (1.13)).

$$B=(1+|m|)/2\Gamma\left(\frac{3}{2}-\frac{|m|}{2}\right)\Gamma\left(\frac{3}{2}+\frac{|m|}{2}\right),$$

$$m=\frac{d\log \Phi_1(\ln \tau)}{d\log \tau},$$

where the sabscripts 0 and 2 indicate the order of approximation. As can be seen from Fig. (1.8) a good agreement is obtained among the values calculated from these equations.

Rate process of dielectric relaxation[4,9~12]

According to the theory of absolute reaction rate the average time required for a single rotation of dipole, i.e., the average relaxation time τ_0, is written as

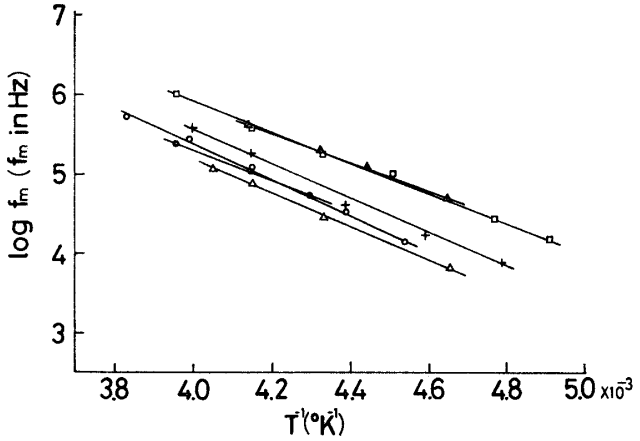

Fig. 1.9. Plots of log f_m against T^{-1} for absolutely dried woods. (open and closed circles: HOONOKI (L), open triangles: KEYAKI (L), crosses: SUGI (L), closed triangles: KEYAKI (T), squares: HINOKI (T)).

Table 1.4. Values of ΔE, ΔH, ΔF and ΔS for absolutely dried woods.

Species	D	T (°C)	ΔE	ΔH	ΔF	ΔS
			(kcal/mole)			(cal/mole·deg.)
HINOKI	T	−69 ~−10	9.8	9.3	7.1~7.2	9~10
SUGI	L	−64 ~−10	9.6			
HOONOKI	L	−53 ~−12	10.2			
	L		8.5			
	θ=30°		8.1			
	45	−50~20	8.0			
	70		7.7			
	R		7.7			
	L	−40~53	8.7			
KEYAKI	T	−58 ~−32	8.5			
	L	−58 ~−12	9.6			

$$\tau_0 = \frac{h}{kT} \exp\left(\frac{\Delta F}{RT}\right), \tag{1.17}$$
$$\Delta F = \Delta H - \Delta ST,$$

where h the PLANCK onstant, k the BOLZMANN constant, R the gas constant, T the absolute temperature, ΔF the free energy of activation, ΔH the heat of activation and ΔS the entropy of activation respectively. If m is the slope of $\log \tau_0^{-1}$ versus T^{-1} curve, ΔH is given by (2.303Rm − RT), in which the first term 2.303Rm is termed the apparent energy of activation ΔE. Then, ΔS can be calculated from[13]

$$\Delta S = 2.303R\left(\log\frac{1}{\tau_0} - \log\frac{kT}{h} + \frac{m}{T}\right) - R. \tag{1.18}$$

Fig. (1.9) shows the plot of log f_m, in which f_m is the frequency corresponding to ϵ''_m, against the resiplocal of absolute temperature T^{-1} for absolutely dried woods. The values of ΔE, ΔH, ΔF and ΔS calculated by Eqs. (1.17) and (1.18) are listed in Table (1.4).

1.2 Relaxation mechanism

As shown in the preceding section, a dielectric relaxation process occurs in absolutely dried wood. In this section, in order to make clear the mechanism of this relaxation process the dielectric properties of wood constituents including cellulose, mannan, xylan and lignin will be discussed.

Dielectric absorption of cellulose and hemicelluloses

The existence of a relaxation process in dry cellulose has been shown by many workers. These workers include KRÖNER[14], TRAPP[15], MUUS[16], CARKINS[17], ISHIDA[18] and MIKHAILOV[19]. For instance TRAPP and coworker[15] have reported that a dielectric relaxation process occurs in dry cellulose in the frequency range of 10^7 to 10^8 Hz at room temperature. MUUS[16] has measured the dielectric properties of cellophane and scoured cotton and detected two absorptions without maximum in the frequency range from 0.1 to 100 kHz. He ascribes these absorptions to the orientation polarization of hydroxyl group in the crystalline and noncrystalline regions of cellulose respectively. ISHIDA and coworkers[18] have investigated the dielectric properties of three cellulose fibers and suggested that the dipoles in the noncrystalline region and on the surface of the crystalite provide the chief contribution to the relaxation process since the order of the magnitude of $(\epsilon_0 - \epsilon_\infty)$for the samples parallels that of their water vapor accessibilities. MIKHAILOV and coworkers[19] ascribe this relaxation to a movement of methylol group in the noncrystalline region. FUKADA[20] has determined the temperature dependence of piezoelectric, viscoelastic and dielectric properties for dry wood. According to this author the relaxation process occurred at about −100°C and 50 Hz results from the tortional vibrations of cellulose molecules.

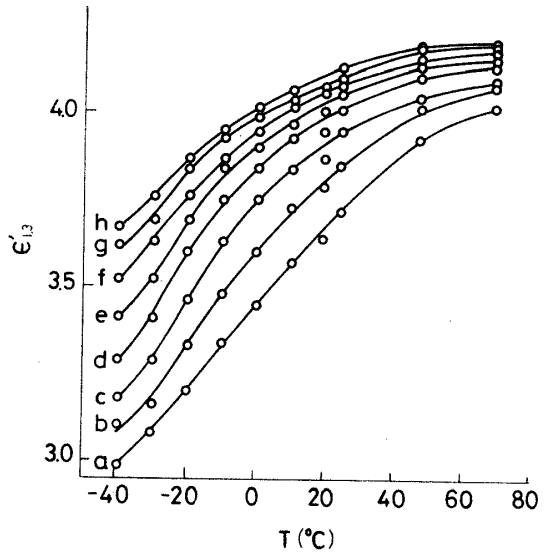

Fig. 1.10. Temperature dependence of $\epsilon'_{1.3}$ at various frequencies for dry Whatman cellulose. (m.c.=0.3 %, γ=1.3, a : 1 MHz b : 300 kHz c : 100 kHz d : 30 kHz e : 10 kHz f : 3 kHz g : 1 kHz h : 300 Hz).

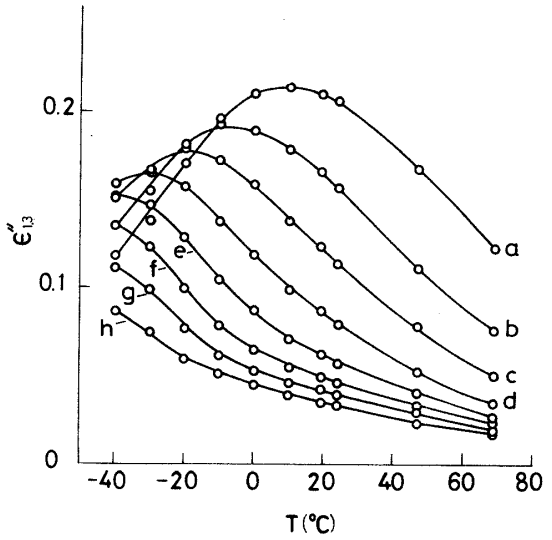

Fig. 1.11. Temperature depencence of $\epsilon''_{1.3}$ at various frequencies for dry Whatman cellulose. (m.c.=0.3 %, γ=1.3, a : 1 MHz b : 300 kHz c : 100 kHz d : 30 kHz e : 10 kHz f : 3 kHz g : 1 kHz h : 300 Hz).

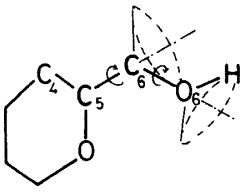

Fig. 1.12. A mode of molecular motion for methylol group in a glucose residue.

In Figs. (1.10) and (1.11) the $\epsilon'_{1.3}$ and $\epsilon''_{1.3}$ curves for cellulose as a function of temperature at each frequency are shown. As is observed in these figures, a relaxation process occurs in the dry state. When log f_m is plotted against T^{-1}, a linear relationship is obtained as shown in Fig.(1.26). The ΔE values calculated are about 10[12] and 11.7 kcal/mole[37].

Fig. (1.12) illustrates a mode of molecular motion for methylol group in a glucose residue. ZHBANKOV[21] has reported that the O_6 atom in methylol group has three stable positions, i.e., at 80, 177 and 300 degrees clockwise from the cis-position of the O_6 and C_4 atoms, and the heights of the energy barrier between these positions are about 3 to 10 kcal/mole. These values compare fairly well with those obtained experimentally.

On the other hand, it has been reported that two dispersions occur in the dielectric measurement for solution of isobutyl alcohol in viscous oil. HÄFELIN attributes

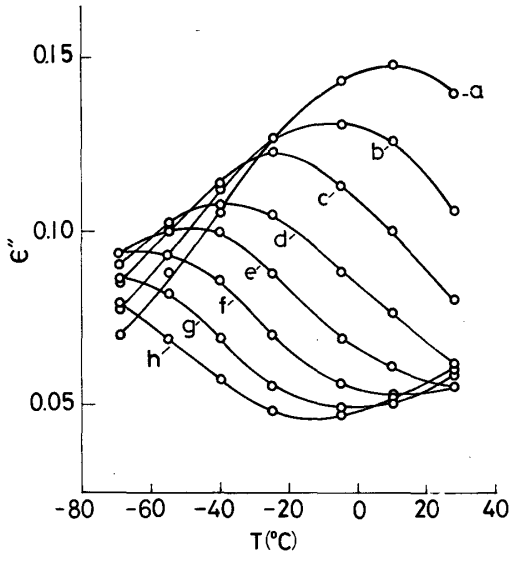

Fig. 1.13. Temperature dependence of ϵ'' at various frequencies for dry mannan. (a : 1 MHz b : 300 kHz c : 100 kHz d : 30 kHz e : 10 kHz f : 3 kHz g : 1 kHz h : 300 Hz).

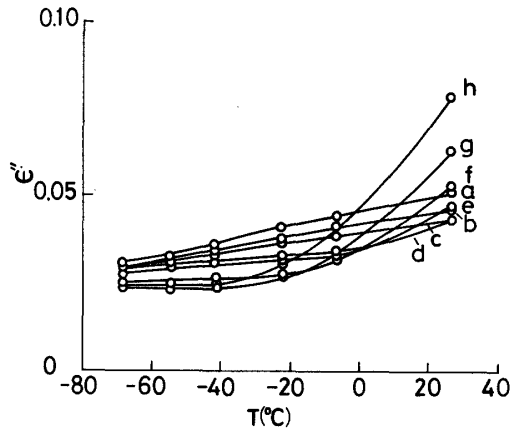

Fig. 1.14. Temperature dependence of ϵ'' at various frequencies for dry beech mannan. (a : 1 MHz b : 300 kHz c : 100 kHz d : 30 kHz e : 10 kHz f : 3 kHz g : 1 kHz h : 300 Hz).

the dispersion in the higher frequency range to the rotation of methylol group[22]. This fact suggests that methylol group can be an orienting unit.

In Figs.(1.13) and (1.14) the ϵ'' versus T curves for mannan and xylan are shown. The locations of loss peak maxima for mannan in which methylol group is present compare fairly well those for cellulose. The ΔE value calculated is 9.2 kcal/mole. This relaxation process, however, can not be detected in xylan in which methylol group is absent. These facts suggest that the relaxation process occurred in both cellulose and mannan may be associated with methylol group.

Recently SAWATARI and coworkers[23] have measured the dielectric properties of triphenylmethylcellulose and cellulose acetate with various degrees of substitution. They suggest that the relaxation mechanism occurred in cellulose is related to a motion of methylol group since the absorption intensity decreases with increasing degree of substitution. On the other hand, it has been reported that a similar relaxation process occurs in the mechanical measurements for cellulose[24,25]. For instance KIMURA and others have studied the mechanical properties of cellulose as well as hemicelluloses by means of the tortional vibration. They suggest that the relaxation process occurred at $-100°C$ and in 0.2 to 2Hz for cellulose is due to a motion of methylol group by comparing with the results for triphynylmethylcellulose.

Thus, from these results and the result on the relationship between dielectric

properties and crystallinity of cellulose on which will be discussed in the next paragragh, it may be concluded that the dielectric relaxation process occurred in dry cellulose is associated with the orientation polarization of methylol dipole in the noncrystalline region.

Dielectric properties and crystallinity of cellulose

If the relaxation process occurred in dry cellulose is associated with a motion of methylol group in the noncrystalline region, then it may be expected that the extent of the dielectric dispersion is directly related to the quantity of noncrystalline fraction.

Numerous workers have studied the correlation between the dielectric properties and the noncrystalline content for celluloses. These workers include CARKINS[17], VERSEPUT[27], KANE[28], ISHIDA[18], PANDE[29] and VENKATESWARAN[30]. For instance CALKINS[17] has measured the dielectric constant as a function of moisture regain for regenerated celluloses and found a linear relationship between them. VERSEPUT[27] has measured the dielectric constant at 1×10^3Hz and 30°C for several cellulose fibers to examine the relationship between the dielectric properties and the crystallinity, and showed that, although the amount of the polarization is not necessarily entirely dependent upon the quantity of noncrystalline region, a certain amount of the polarization seems to be due to the rotational vibration of cellulose chains in the noncrystalline region since the dielectric constant of cellulose is profoundly influenced by the crystallinity. KANE[28] has studied the relationship between the intrinsic dielectric constant and the water vapor accessibility of six celluloses and obtained the following linear equation.

$$\epsilon_C=8.60\delta_A+3.88\delta_C, \quad \text{at } 10\,\text{kHz and } 30°\text{C}, \tag{1.19}$$

where ϵ_C is the intrinsic dielectric constant of cellulose, and δ_C and δ_A are the inaccessible and accessible fractions, respectively. According to this equation, the dielectric constants of the accessible and inaccessible celluloses are 8.60 and 3.88, respectively. ISHIDA and coworkers[18] have measured the dielectric constant and loss factor for three cellulose fibers in the dry condition over the frequency range from 5×10^2 to 3×10^6Hz and the temperature range from -60 to 20°C. They show that the value of $(\epsilon_0-\epsilon_\infty)$determined from the COLE-COLE plots, which are proportional to the concentration of dipoles contributing to the orientation polarization, increase with increasing accessibility of the samples. VENKATESWARAN[30] has investigated the relationship between the intrinsic dielectric constant and the crystallinity index calculated from the X-ray measurements for cotton linters, bleached sulphite pulp and ramie treated with various concentrations of ethylamine, and found that there is an excellent linear correlation between them at any frequency. Thus, the dielectric constant of cellulose can be thought as that of a two component system, i.e., one

component the crystalline cellulose and the other the noncrystalline cellulose.

According to the phenomenological theory of dielectrics, the dispersion magnitude $(\epsilon_0-\epsilon_\infty)$ can be written as

$$\epsilon_0-\epsilon_\infty=\frac{2}{\pi}\int_{-\infty}^{\infty}\epsilon''(\omega)\,\mathrm{d}\ln\omega, \tag{1.20}$$

where ϵ_0 and ϵ_∞ are the static dielectric constant and the dielectric constant at very high frequencies at which the orientation of any dipole is impossible respectively, and $\epsilon''(\omega)$ is the dielectric loss factor as a function of angular frequency ω. SILLARS[31] has derived the following relation by generalizing the DEBYE formula.

$$\int_{-\infty}^{\infty}\epsilon''\mathrm{d}\ln\omega=\int_{-\infty}^{\infty}\left\{C\int\frac{\omega\tau}{1+\omega^2\tau^2}G(\tau)\,\mathrm{d}\tau\right\}\mathrm{d}\ln\omega=\frac{C\pi}{2}n, \tag{1.21}$$

where

$$C=\frac{4\pi}{3}\cdot\frac{(\epsilon_0+2)^2}{3}\cdot\frac{\mu^2}{3kT},$$

n the number of polar molecules per c.c., μ the dipole moment, k the Bolzmann constant, T the absolute temperature, τ the relaxation time, $G(\tau)\mathrm{d}\tau=\mathrm{dn}$, respectively. This equation shows that if $\epsilon''(\omega)$ is plotted against $\ln\omega$ the total area under the curve is propotional to the total concentration of dipoles. Employing this method, NAKAJIMA and SAITO[32] has found a linear relationship between the area under the ϵ'' versus log $(\omega/2\pi)$ curve and the amount of noncrystalline region estimated from density for the low temperature dispersion of polymonochlorotrifluoroethylene. Furthermore, they have discussed the correlation between $(\epsilon_0-\epsilon_\infty)$ determined from the COLE-COLE plots and the crystallinity for the α and β absorptions of polyethylene terephlalate[33].

From Eqs. (1.20) and (1.21), the following relation is derived.

$$\epsilon_0-\epsilon_\infty=cn. \tag{1.22}$$

Here, if it is assumed that ϵ_∞ is constant regardless of degree of crystallinity, then ϵ' is propotional to the concentration of the dipole contributing to the orientation polarization, i.e., the quantity of noncrystalline fraction, since it is considered that ϵ' is nearly equal to ϵ_0 in low frequency range and that the dipoles in the noncrystalline region make a substantial contribution to the orientation polarization.

On the other hand, PANDE[29] has derived theoretically the following linear relationship between ϵ' and the volume fraction of crystallinity δ_C for cellulose from the MAXWELL relation and the GLADSTONE-DALES law.

$$\epsilon'\simeq C_1\delta_C+C_2, \tag{1.23}$$

$$C_1=2(\rho_C-\rho_A)\frac{n-1}{\rho}\left(1+\frac{n-1}{\rho}\cdot\rho_A\right),$$

$$C_2=\left(1+\frac{n-1}{\rho}\cdot\rho_A\right)^2,$$

where n the average refractive index, ρ_C and ρ_A the densities of the crystalline and noncrystalline regions, ρ the average density of the substance, respectively.

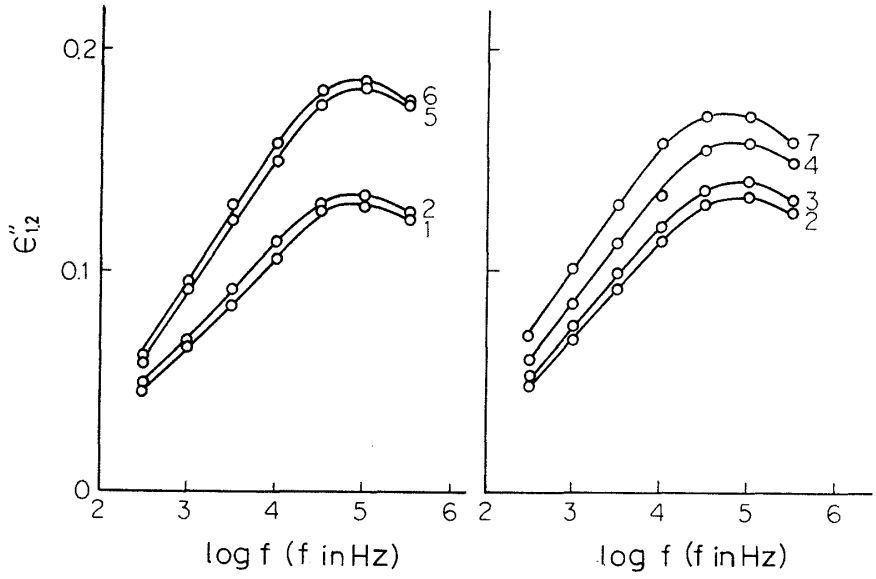

Fig. 1.15. Frequency dependence of $\epsilon''_{1.2}$ at $-32°C$ for absolutely dried celluloses. ($\gamma=1.2$, 1 : cotton 2 : Whatman cellulose 3 : Whatman cellulose ground in a ball mill for 15 mins. 4 : Whatman cellulose ground for 30 mins. 5 : Avicel 6 : Merck cellulose 7 : Whatman cellulose ground for 1 hr.)

In Fig. (1.15) the loss factor $\epsilon''_{1.2}$ for cellulose powders shown in Table (1.5) at $-32°C$ computed to the standard density 1.2 as a function of log f is illustrated. The data show that the loss factor of cellulose I goes through a maximum at 1×10^5 Hz. The same trend is also observed in cellulose II. The $\epsilon''_{1.2}$ value for Whatman celluloses increases in magnitude with increasing prolonged grinding in a ball mill, i.e., with decreasing degree of crystallinity.

In Fig. (1.16) the dielectric constant $\epsilon'_{1.2}$ as a function of crystallinity index CI for cellulose I is shown. Here, CI is calculated from[34]

$$CI=\frac{(I_{002}-I_A)}{I_{002}}\times 100,$$

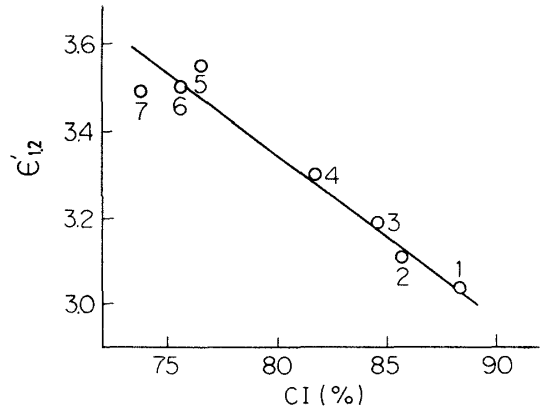

Fig. 1.16. $\epsilon'_{1.2}$ versus crystallinity index curve for absolutely dried celluloses (see Table 1.5).

where I_{002} is the maximum intensity of the (002) lattice diffraction and I_A is the intensity of diffraction in the same units at $2\theta = 18$ degree. The equation determined by a statistical analysis of the experimental results is shown as

$$\epsilon'_{1.2} = -3.75 \times 10^{-2} CI + 6.33, \quad \text{at 1 kHz and } -32°C, \quad |r| = 0.973.$$

According to this equation, the values of the intrinsic dielectric constants for the non-crystalline and crystalline celluloses are 8.06 and 3.10 at 1kHz and $-32°C$ respectively. In Fig. (1.17) $\epsilon'_{1.2}$ as a function of sorption ratio SR for cellulose I is shown. Here, SR is defined as the ratio of sorption of a cellulose to that of cotton under the same conditions and is determined at 63.5%R.H. and 20°C since it has been reported that humidity of 60 to 85% would be suitable for the determination of crystallinity.

Table 1.5. Values of CI, SR, ($\epsilon'_{1.2}$) 1kHz and CW for cellulose samples.

No.	Samples	CI (%)	SR	($\epsilon'_{1.2}$) 1kHz	α'	CW (Å)*
1	Cotton treated with 3% HCl	88.4	1.000	3.04	0.304	69
2	Whatman cellulose	85.7	1.025	3.11	0.300	66
3	Whatman cellulose ground for 15 mins.	84.6	1.027	3.19	0.289	66
4	Whatman cellulose ground for 30 mins.	81.7	1.119	3.30	0.279	64
5	Avicel	76.5	1.252	3.55	0.302	46
6	Merck cellulose	75.6	1.225	3.50	0.299	44
7	Whatman cellulose ground for 1 hr.	73.8	1.326	3.49	0.274	60
8	Whatman cellulose treated with 17.5% NaOH (cellulose II)	—	1.871	3.67	0.289	—
9	Cotton treated with 3% HCl and then 17.5% NaOH (cellulose II)	—	1.873	3.68	0.280	—

* Crystalline width CW is calculated from the (002) diffraction by using the Scherrer equation.

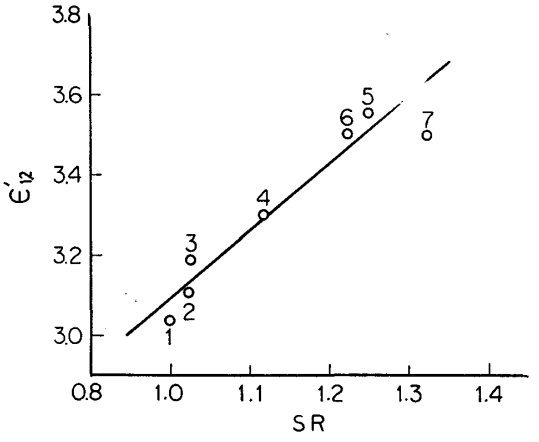

Fig. 1.17. $\epsilon'_{1.2}$ versus sorption ratio curve for absolutely dried celluloses (see Table (1.5)).

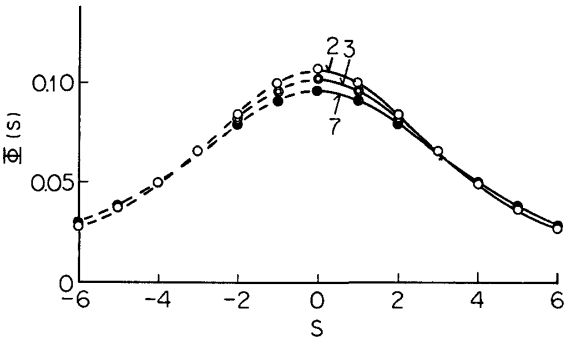

Fig. 1.18. Distribution function of relaxation times at $-32°C$ for absolutely dried Whatman cellulose. ($\gamma = 1.2$, 2 : control 3 : ground in a ball mill for 15 mins. 7 : ground for 1 hr.).

Furthermore, SR is independent of temperature and relative humidity over a wide range of the conditions[35] and is related with the quantity of noncrystalline fraction for cellulose by $F_A = SR/2.60$[36].

Table (1.5) shows the values of CI, SR, $\epsilon'_{1.2}$, α' and the crystalline width D for the cellulose samples used. In Fig. (1.18) the distribution function of relaxation times $\Phi(s)$ calculated from Eq. (1.13) for Whatman celluloses is shown. As can be seen from this figure, the distribution of relaxation times seems to become somewhat wider by prolonged grinding in a ball mill. Furthermore, it is considered that the distribution of relaxation times for cellulose II is generally wider compared with that for cellulose I, since the value of α' for cellulose II is less than that for cellulose I.

Dielectric properties of cellulose irradiated with gamma rays[37]

It has been reported that high energy irradiation of cellulose results in the random chain cleavage at nearly the same rate in the crystalline and noncrystalline regions[38], the formation of carbonyl and carboxyl groups as a result of oxidization[39, 40] and the reduction in crystallinity[41]. In this paragraph, the effects of gamma radiation from ^{60}Co (dose rate: 3.20 Mrad/hr, dosage: 0 to 321 Mrad) on the dielectric properties of cellulose will be discussed.

Fig. (1.11) shows the relationship between $\epsilon''_{1.3}$ (the subscript 1.3 implies specific gravity) at various frequencies and temperature for untreated cellulose. The occurrence of a single relaxation process is evident within the experimental temperature range at each frequency. As the frequency decreases, the locations of the loss peaks move to lower temperature region with decrease of peak height. Fig. (1.19) shows the contour diagram of $\epsilon''_{1.3}$ as a function of temperature and logarithmic frequency for untreated cellulose. As has already been discussed, this relaxation process is associated with a motion of methylol group in the noncrystalline region. In Fig. (1.20) the frequency dependence of $\epsilon'_{1.3}$ and $\epsilon''_{1.3}$ at $-24°C$ for cellulose irradiated with gamma rays is shown. The values of $\epsilon'_{1.3}$ and $\epsilon''_{1.3}$ start to increase at the irradiation levells in excess of 29 Mrad and reach a maximum at around 97 Mrad, and then decrease rapidly with increase of irradiation dosage. At the dosage of 321 Mrad the $\epsilon''_{1.3}$ versus log f curve is very broad. The COLE-COLE plot of the results in Fig. (1.20) is shown in Fig. (1.21). As is evident from this figure, the COLE-COLE law can be satisfactorily applied to the data obtained in the whole range of dosage tested. The parameters $(\epsilon_0 - \epsilon_\infty)$ and $(1-\alpha)$ determined from Fig. (1.21) are plotted against logarithmic irradiation dosage log D in Fig. (1.22). The value of the increment $(\epsilon_0 - \epsilon_\infty)$ remains unchanged up to 1×10^7 rad and reaches a maximum at 1×10^8 rad and then starts to decrease rapidly with increase of D. On the other hand, the value of $(1-\alpha)$ decreases slowly with dosage up to 1×10^8 rad

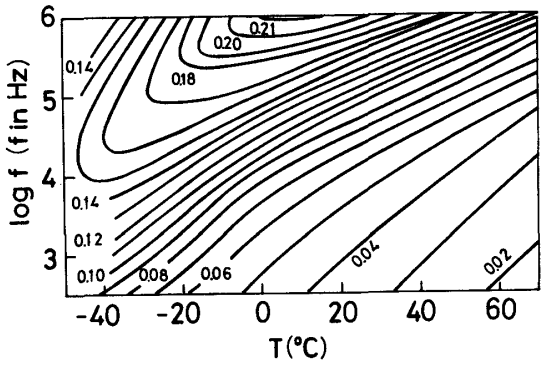

Fig. 1.19. Contour diagram of dielectric loss factor $\epsilon''_{1.3}$ as a function of temperature and frequency for dry Whatman cellulose. (m.c.=ca. 0.3 %, γ=1.3).

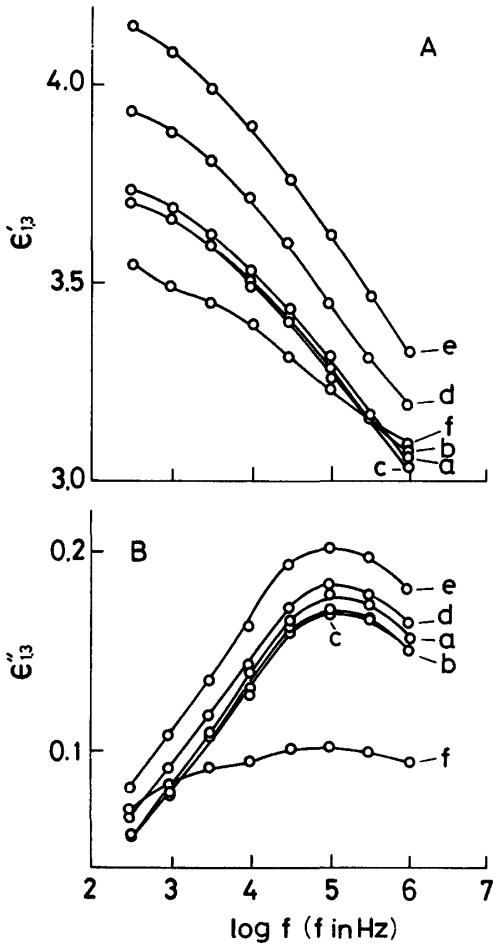

Fig. 1.20. Frequency dependence of dielectric constant (A) and loss factor (B) at −24°C for absolutely dried Whatman cellulose irradiated with gamma rays. a: control b: dosage 3.2 Mrad c: 9.6 Mrad d: 29 Mrad e : 97 Mrad f: 321Mrad).

and then decreases rapidly. This result indicates that the distribution of relaxation times becomes wider with irradiation dosage.

In Figs.(1.23)and(1.24)the temperature dependence of $\epsilon''_{1.3}$ at various frequencies for cellulose irradiated at dosage of 97 and 321 Mrad is illustrated. The solid and dotted lines in Fig.(1.23) represent the results of the samples containing about 0.3% moisture and after drying, respectively. Comparing these results with that in Fig. (1.11), it can be seen that the adsorbed moisture gives rise to an additional relaxation process in the irradiated samples. This relaxation process, however, eliminates completely by drying as shown by the dotted lines in the figure. Therefore, it may be supposed that the relaxation process is closely associated with the adsorbed water. On the other hand, the loss peak due to a motion of methylol group increases

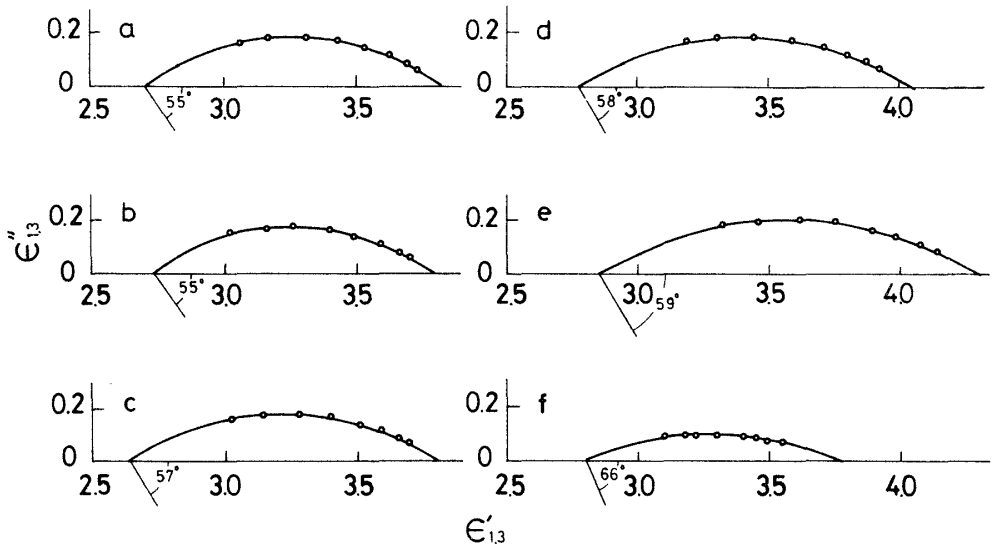

Fig. 1.21. COLE-COLE plots for absolutely dried Whatman cellulose irradiated with gamma rays. (a : control b : dosage 3.2 Mrad c : 9.6 Mrad d : 29 Mrad e : 97 Mrad f : 321 Mrad).

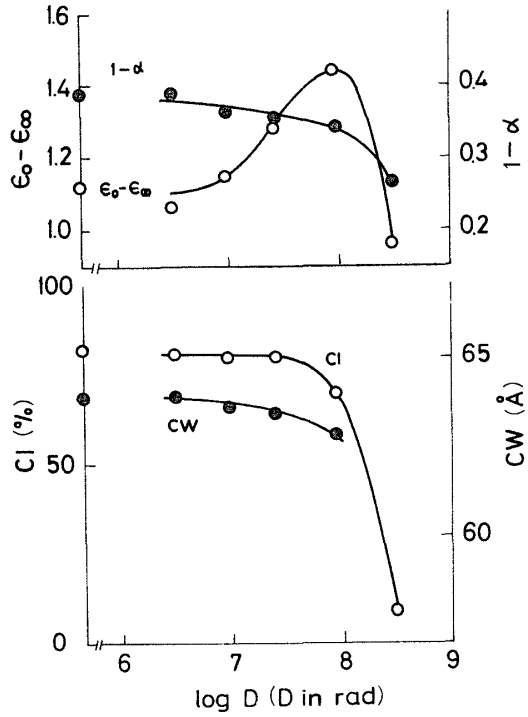

Fig. 1.22. $(\epsilon_0-\epsilon_\infty)$, $1-\alpha$, CI and CW of Whatman cellulose as a function of logarithmic irradiation dosage.

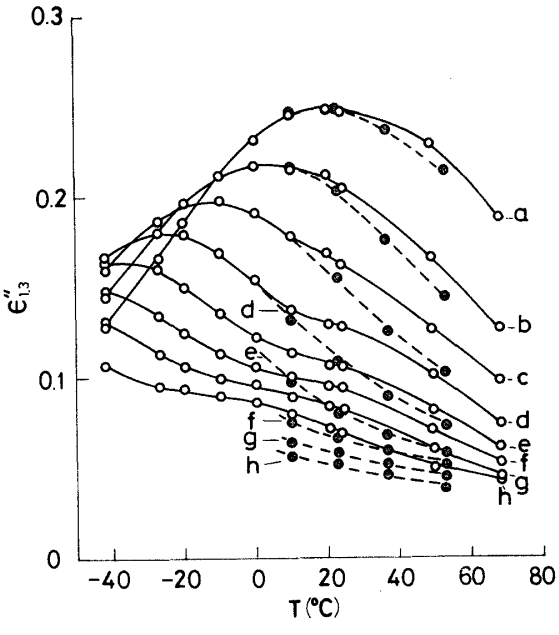

Fig. 1.23. Temperature dependence of dielectric loss factor at various frequencies for Whatman cellulose irradiated with gamma rays at a dosage of 97 Mrad. (solid lines : m.c. = ca. 0.3%, dotted lines: m.c. = 0%, a : 1 MHz b : 300 kHz c : 100 kHz d : 30 kHz e : 10 kHz f : 3 kHz g : 1 kHz h : 300 Hz).

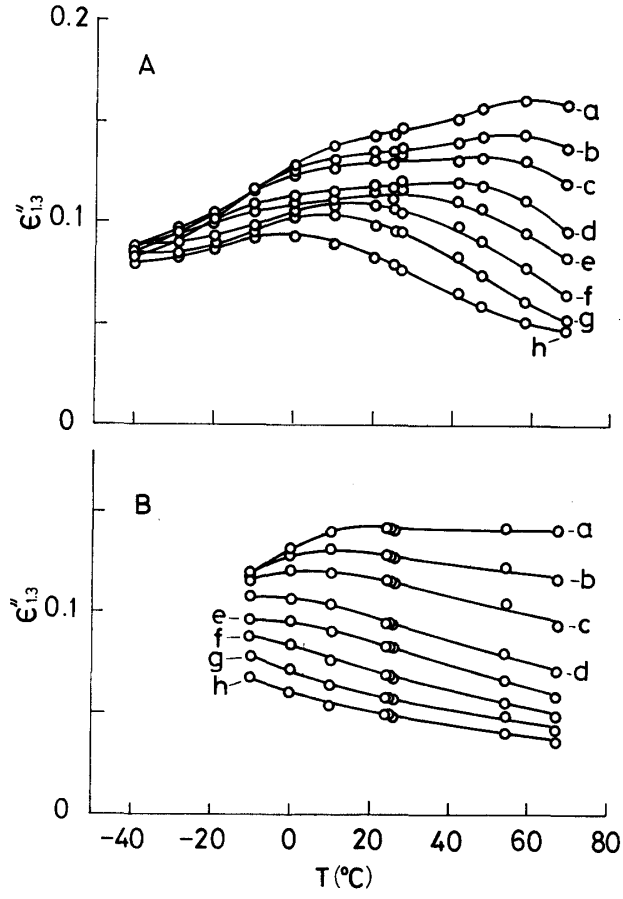

Fig. 1.24. Temperature dependence of dielectric loss factor at various frequeccies for Whatman cellulose irradiated with gamma rays at a dosage of 321 Mrad. (A: m.c.=ca. 0.3%, B: m.c.=0%, a: 1 MHz b: 300 kHz c: 100 kHz d: 30 kHz e: 10 kHz g: 1 kHz h: 300 Hz).

in height and the location of the peak moves slightly to higher temperature range compared with that in Fig. (1.11). At the dosage of 321 Mrad, the loss peak due to a motion of methylol group decreases rapidly compared with those in Figs. (1.11) and (1.23), while the peak due to the adsorbed water increases in height but it is almost elminated by drying as shown in Fig. (1.24B).

Thus, the relaxation process due to the adsorbed water is brought about by the irradiation. The influence of water on the loss factor for cellulose irradiated with gamma rays is very similar to that on the β relaxation for polyamides and polyurethanes[42] which is suggested by ILLERS[43] to be due to a motion of water-carbonyl group complex. BLOUIN and coworker[39] have shown that gamma irradiation of cellulose results in the formation of carbonyl and carboxyl group and the difference in the infra-red spectral curves of the irradiated samples from the control curve is the appearance of an absorption band at 5.75 μ which is assigned to the C=O streching band. As shown in Fig. (1.25) which illustrates the infra-red

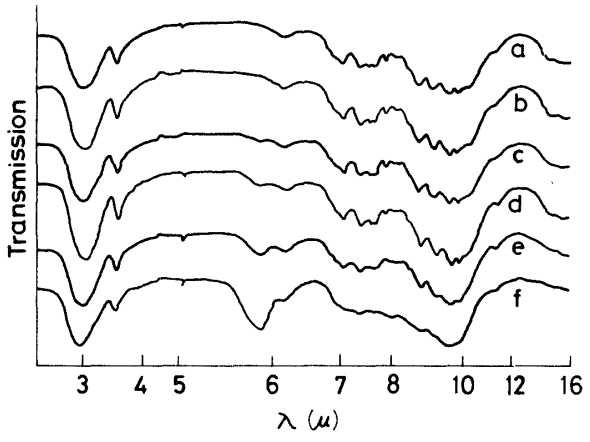

Fig. 1.25. Infra-red spectra of Whatman cellulose irradiated with gamma rays. (a : control b : 3.2 Mrad c : 9.6 Mrad d : 29 Mrad e : 97 Mrad f : 321 Mrad).

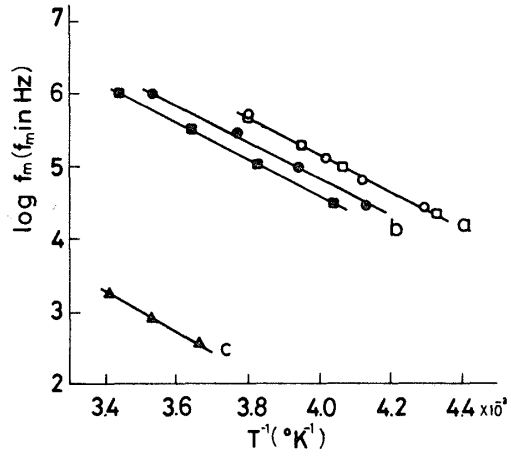

Fig. 1.26. Frequency-temperature location of dielectric loss factor maxima for Whatman cellulose irradiated with gamma rays. (f_m is determined from $\epsilon''_{1.3}$ versus T curves in (a) and (c), and from $\epsilon''_{1.3}$ versus T curves in (b), circles : control squares : 97 Mrad closed triangles : the relaxation due to the orientation of water molecules adsorved to carbonyl group).

spectra for cellulose irradiated with gamma rays, the absorption intencity at 5.8 μ increases with irradiation dosage. This tendency parallels that of the dielectric absorption associated with water. As the dissociation energy for hydrogen bond between water molecule and carbonyl group is greater than that between water molecule and alcoholic hydroxyl group, it may be supposed that the relaxation time for the reorientation of water molecules adsorbed to carbonyl group is longer than that to alcoholic hydroxyl group. Thus, the relaxation process associated with a motion of water-carbonyl complex may occur in lower frequency range compared with that of water-alcoholic hydroxyl group complex. In this connection, it has been reported that the relaxation process associated with the water adsorbed to alcoholic hydroxyl group occurs at 1kHz and about $-80°C$[44], while that of free water at around 15 GHz[45].

In Fig. (1.26) $\log f_m$ for the untreated and irradiated samples is plotted against T^{-1}. The values of ΔE calculated from the curves (a), which are the apparent energy of activation for a motion of methylol group, are 11.7 kcal/mole. The ΔE value for the relaxation due to the orientation of water adsorbed to carbonyl group, which is calculated from the curve (c), is about 13 kcal/mole. This value compares well with those of 14.5 and 13 kcal/mole for the β relaxation process in polyamides [42,43].

In Fig. (1.22) the crystalline index CI and the crystalline width CW are plotted against log D. The CI value remains almost unchanged up to 3×10^7 rad and starts to decrease rapidly at about 1×10^8 rad, and then falls to 9% at 321 Mrad. Similar tendency can also be detected in the infra-red spectra shown in Fig. (1.25) in which a broadening of the so called crystalline bands in the 7.0 through 9.5μ region occurs at 97 Mrad. On the other hand, the CW value decreases slowly with irradiation dosage.

From these results the effects of gamma radiation on the dielectric properties of cellulose are summarized as follows: Up to a dosage of 1×10^7 rad, no significant change in the dielectric properties take place. Irradiation to a dosage of 3×10^7 rad produces a slight increase in the value of $(\epsilon_0-\epsilon_\infty)$ but little change in the degree of crystallinity. This may suggest that the number of methylol group contributing to the orientation increases mainly in the noncrystalline region. At irradiation levels in excess of 3×10^7 rad a definite reduction in the degree of crystallinity is observed. And the value of $(\epsilon_0-\epsilon_\infty)$ reaches a maximum at around 1×10^8 rad, and this may suggest that the number of methylol group contributing to the orientation increases both in the noncrystalline and crystalline regions. Irradiation above 1×10^8 rad induces a rapid decrease in the value of $1-\alpha$, $(\epsilon_0-\epsilon_\infty)$ and the degree of crystallinity. This may suggest that the number of methylol group decreases as a result of oxidization. On the other hand, by irradiation another dielectric relaxation process occurs in low frequency range at room temperature, and it is estimated that this

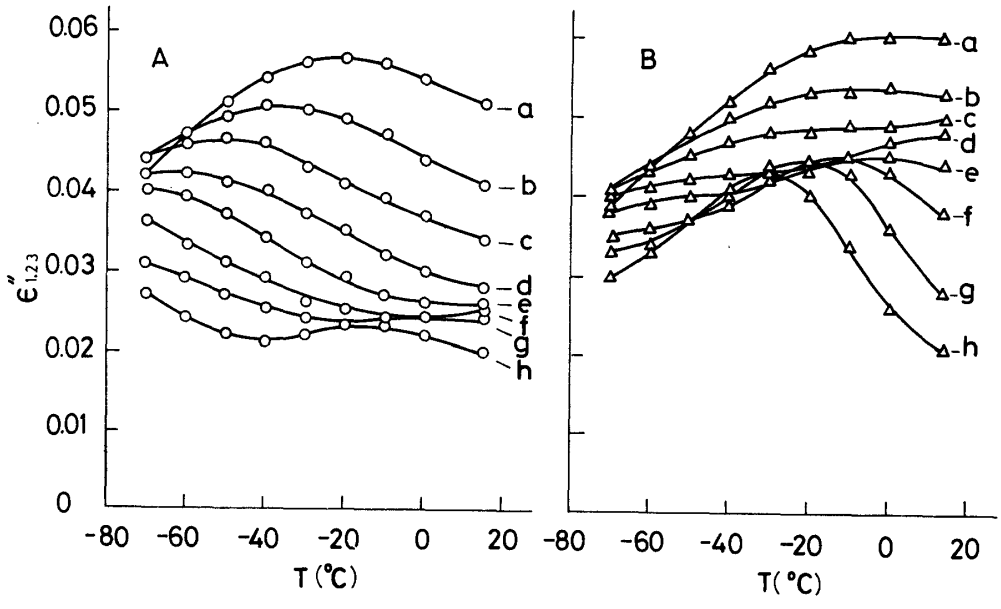

Fig. 1.27. Temperature dependence of $\epsilon''_{1.23}$ at various frequencies for MWL. (γ=1.23, number average molecular weight $\overline{M}n$=2320, A : m.c.= 0.2% B : m.c.=0.8%).

Dielectic absorptions of lignin[47]

Very little work has been reported in the literature on the dielectric properties of lignin. Lignin has many kinds of polar group contributing to the dielectric absorption.

In Figs. (1.27A) and (1.27B) the $\epsilon''_{1.23}$ (the subscript 1.23 implies specific gravity) process is probably due to the orientation of the water adsorbed to carbonyl group. versus T curves at various frequencies for HINOKI MWL (milled wood lignin) containing 0.2% and 0.8% water are illustrated. Furthermore, in Fig. (1.28) the contour diagrams of $\epsilon''_{1.23}$ for the same samples are illustrated. As can be seen from these figures, two absorptions occur within the experimental temperature range at each frequency, i.e., one occurs in high frequency range below room temperature and the other in low frequency range at room temperature. The absorption in high frequency range is not affected by the addition of water, while that in low freq-

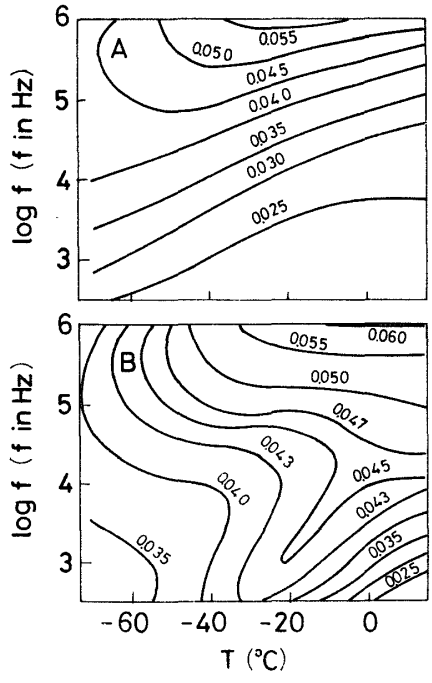

Fig. 1.28. Contour diagram of $\epsilon''_{1.22}$ as a function of temperature and frequency for MWL. (A : m.c.=0.2 %, B : m.c.=0.8 %).

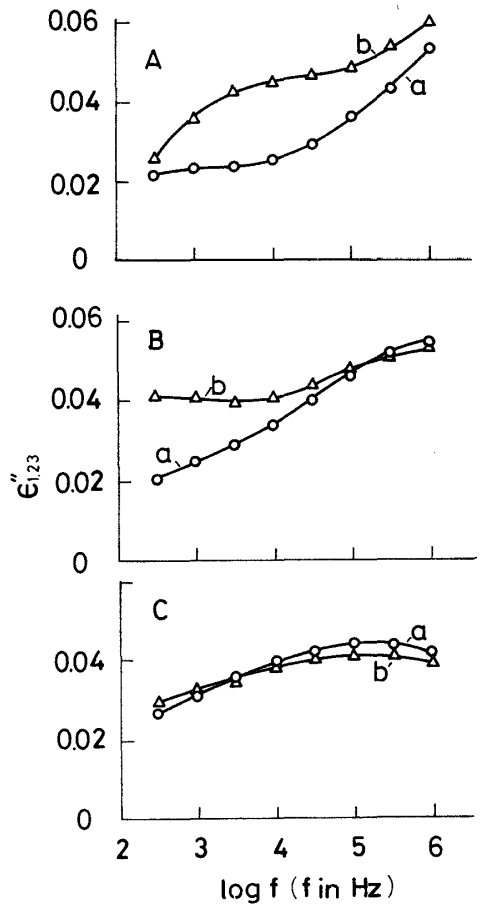

Fig. 1.29. Frequency dependence of $\epsilon''_{1.23}$ for MWL. (a : m.c.=0.2 %, b : m.c.=0.8 %, A : T=0°C B : T=−40°C C : T=−70°C).

uency range is affected remarkably by it. Fig. (1.29) shows the $\epsilon''_{1.23}$ versus log f curves at 0°, −40° and −70°C in which two relaxation processes occur at 0°C in the sample containing 0.8% water, i.e., one in low frequency range and the other in the frequency range higher than 1 MHz, but that in low frequency range scarecely be detected in the sample containing 0.2% water. These absorptions move to lower frequency range with decreasing temperature. At −70°C the peak of the absorption occurring in the frequency range higher than 1 MHz at 0°C can be detected within the experimental frequency range. Here, the plots of log f_m against T^{-1} for these absorptions are linear as shown in Fig. (1.30).

On the other hand, the $\epsilon''_{1.21}$ versus T curves at 300kHz and 1MHz for acetylated MWL together with untreated one are illustrated in Fig.(1.31). As can be seen from this figure, the absorption observed in untreated MWL in high frequency range below room temperature is almost eliminated by acetylation. Therefore, it may be supposed that this absorption is closely associated with hydroxyl groups, i.e., alcoholic and phenolic hydroxyl groups. In this connection, no significant change in the absorption takes place by reducting carbonyl group of MWL by sodium borohydride. Now, in order to make clear the mechanism of this absorption, let us consider the dielectric properties of three kinds of DHP (dehydrogenation polymer)

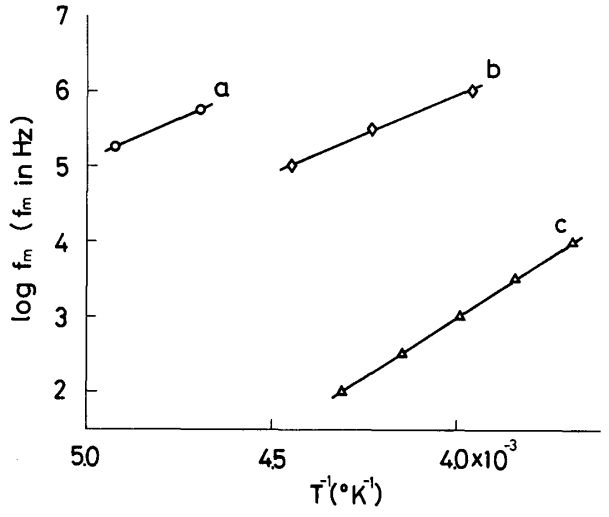

Fig. 1.30. Plots of log f_m against T^{-1} for the relaxation processes in high frequency range (a and b) and in low frequency fange (c) of MWL. f_m is determined from ϵ'' versus log f curves in (a) and from ϵ'' versus T curves in (b) and (c), respectively.

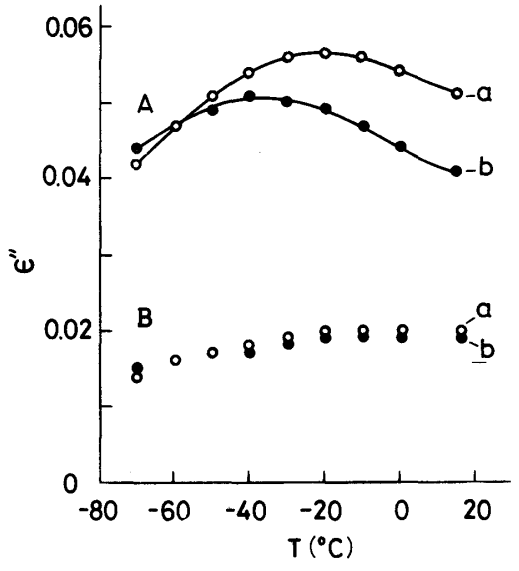

Fig. 1.31. Temperature dependence of ϵ'' at 1 MHz (a) and 300 kHz (b) for MWL (A) and acetylated MWL (B). (B : γ=1.21 m.c.=0.1 % $\overline{Mn}$= 3090).

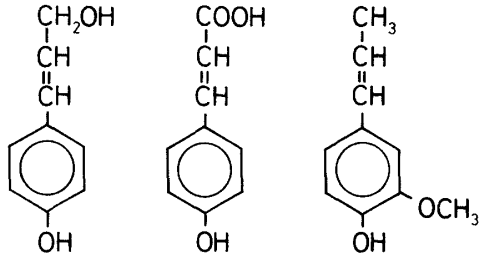

(a) (b) (c)

Fig. 1.32. (a) : p-coumaryl alcohol, (b) : p-coumaric acid, (c) : isoeugenol.

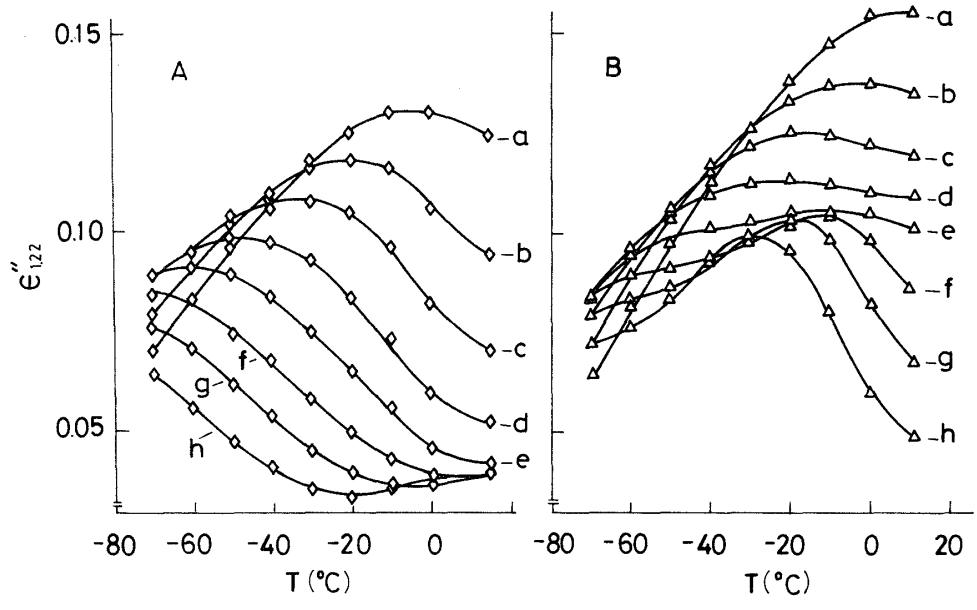

Fig. 1.33. Temperature dependence of $\epsilon''_{1.22}$ at various frequencies for DHP from p-coumaryl alcohol. ($\gamma=1.22$, $\overline{Mn}=607$, A : m.c.$=0\%$ B : m.c.$=1\%$, a : 1 MHz b : 300 kHz c : 100 kHz d : 30 kHz e : 10 kHz f : 3 kHz g : 1 kHz h : 300 Hz).

prepared from p-coumaryl alcohol, p-coumaric acid and isoeugenol, of which structures are shown in Fig. (1.32). Figs. (1.33A) and (1.33B) show the $\epsilon''_{1.22}$ versus T curves at various frequencies for DHPs from p-coumaryl alcohol containing 1 % and 0 % water. Furthermore, Fig. (1.34) shows the $\epsilon''_{1.22}$ versus log f curves at 0°, $-40°$ and $-70°$C for the same samples. The dielectric properties of DHP from p-coumaryl alcohol are very similar to those of MWL. In Fig. (1.35) the polt of log f_m against T^{-1} for the relaxation process in high temperature range below room temperature in DHP from p-coumaryl alcohol is shown. The value of ΔE determined for the absolutely dried sample is 8.7 kcal/mole, which compares fairely well with 9.9 kcal/mole for MWL. On the other hand, Fig.(1.36) shows the ϵ'' versus temperature curves at 100 kHz for DKPs from p-coumaryl alcohol, p-coumaric acid

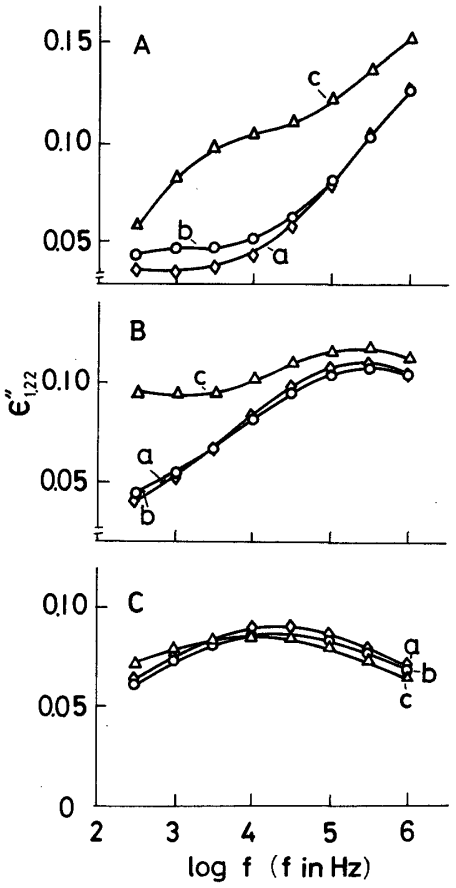

Fig. 1.34. Frequency dependence of $\epsilon''_{1.22}$ at 0°C (A), −40°C (B) and −70°C (C) for DHP from p-coumaryl alcohol. (a : m.c.=0 %, b : m.c=0.2 %, c : m.c.=1 %).

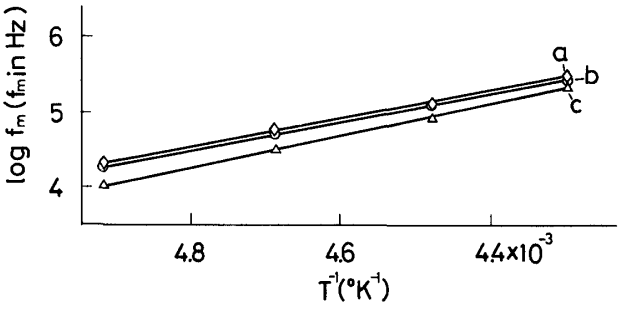

Fig. 1.35. Plots of log f_m against T^{-1} for the relaxation process in high frequency range of DHP from p-coumaryl alcohol. f_m is determined from ϵ'' versus log f curves. (a : m.c.=0 %, b : m.c.=0.2 %, c : m.c.=1 %).

and isoeugenol. The relaxation process occurred in DHP from p-coumaryl alcohol in which methylol group is present does not occur in DHPs from p-coumaric acid and isoeugenol in which methylol group is absent. Concequently from these results it may be concluded that the relaxation process in high frequency range occurred in MWL is associated with the reorientation of methylol group.

Next, let us consider the relaxation process in low frequency range at room temperature which is brought about by the addition of water. Fig. (1.37) shows the frequency and temperature dependences of ϵ'' for DHP from p-coumaryl alcohol due to the adsorbed water only, which is obtained by subtracting the ϵ'' value for the absolutely dried sample from that for the sample containing 1 % water, and the plot of log f_m against T^{-1} for them is illustrated. The value of ΔE is 13.9 kcal/mole, which compares well with 13 kcal/mole for the relaxation process associated with the adsorbed water for cellulose irradiated with gamma rays[37]. As the relaxation

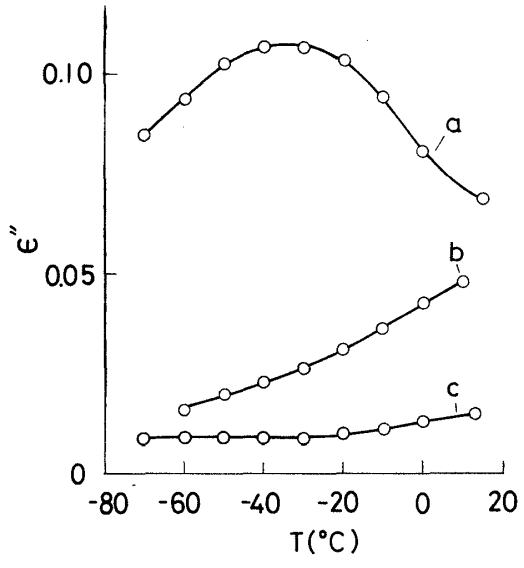

Fig. 1.36. Temperature dependence of ϵ'' at 100 kHz for DHPs from p-coumaryl alcohol (a: m.c.=0%), p-coumaric acid (b: γ=1.01, m.c.=0%, $\overline{Mn}$=1040) and isoeugenol (c: γ=1.10, m.c.=0%, $\overline{Mn}$=1070).

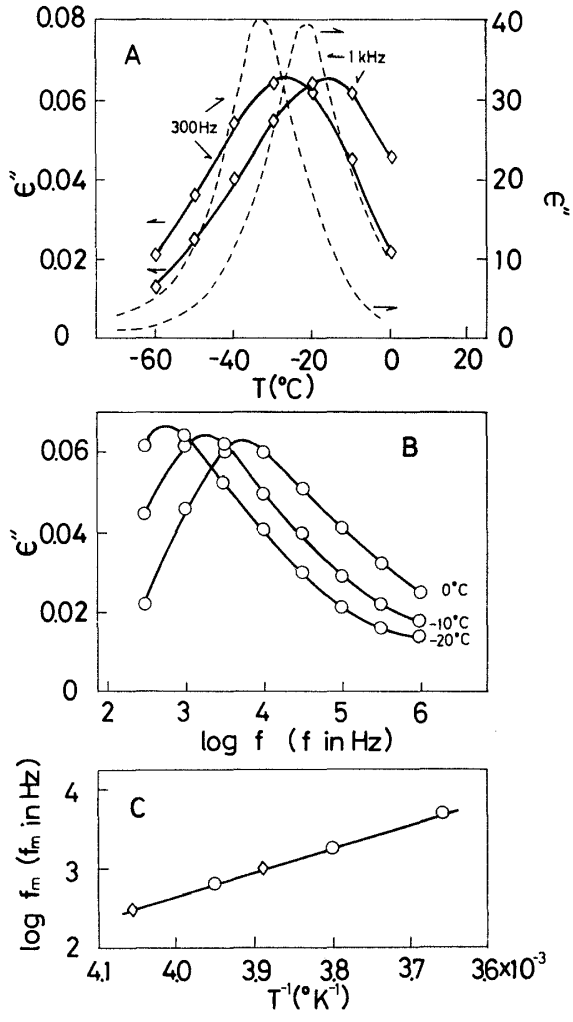

Fig. 1.37. A: Temperature dependence of ϵ'' for the adsorbed water of DHP from p-coumaryl alcohol. Dashed lines represent the results of ice (After SMITH & HITCHCCOK[59]). B: Frequency dependence of ϵ'' for the adsorbed water of DHP from p-coumaryl alcohol. C: Plot of log f_m against T^{-1}.

process associated with the water adsorbed to alcoholic hydroxyl group occurs at 1 kHz and about −80°C[44], so it may be considered that the relaxation process in low frequency range for MWL is associated with the water adsorbed to phenolic hydroxyl group since the force of hydrogen bond between water molecule and phenolic hydroxyl group is greater than that between water molecule and alcoholic hydroxyl group.

Intrinsic dielectric constants of cellulose and lignin

The dielectric constant of a substance itself is termed the intrinsic dielectric

constant[18]. The intrinsic dielectric constant of cellulose has been reported by KANE[28], TRAPP[15], ISHIDA[18] and VENKATESWARAN[30]. For instance KANE[28] has measured the intrinsic dielectric constant of six celluloses using the liquid mixture technique and found a linear correlation between the intrinsic dielectric constant and the water vapor accessibility. The result is shown in Table (1.6). On the other hand, TRAPP and coworker[15] have measured the dielectric constant of a mixed system consisting of cellulose, air and paraffin, and calculated the intrinsic dielectric constant by using the LICHTENECKER-ROTHER formula. ISHIDA and others[18] have also measured the dielectric constant of a mixed system, i.e., cellulose fiber, polyethylene film and air, and calculated the intrinsic dielectric constant of cellulose fibers parallel to the fiber axes. The result for cotton sliver is listed in

Table 1.6. Relationship between accessibility A and intrinsic dielectric constant ϵ_c of cellucloses (After KANE[28]).

Celluloses	A (%)	ϵ_c
Hydrocellulose	34.0	5.49
Cotton linters	42.3	5.86
Wood alpha pulp	42.4	5.86
Bleached sulfite pulp	45.9	6.15
Cellophane	57.0	6.56
Regenerated viscose	83.9	7.86

Table 1.7. Intrinsic dielectric constant of cotton sliver (After ISHIDA *et al.*[18])

T (°C)	3 MHz	1 MHz	300 kHz	100 kHz	30 kHz	10 kHz	3 kHz	1 kHz	330 Hz	$\epsilon_{c\infty}$*
20	4.7	5.4	6.0	6.4	6.7	6.9	7.1	7.2	7.3	4.1
0	4.4	4.8	5.2	5.6	6.0	6.3	6.5	6.7	6.8	3.7

These values at 20°C are determined by the extrapolation.
* $\epsilon_{c\infty}$ is estimated from the COLE-COLE plot.

Table (1.7). VENKATESWARAN[30] has measured the dielectric constant of three cellulosic materials and determined the intrinsic dielectric constant by correcting to the density 1.59. HERMANS and coworker[46] have computed the two principal refractive indices for crystalline native cellulose, i.e., 1.618 and 1.543. According to the Maxwell's relation the square of refractive index is the dielectric constant at optical frequencies, so that the values of the intrinsic dielectric constants in the two principal directions for the ideal cellulose fiber at optical frequencies are 2.618 and 2.381.

On the other hand, VENKATESWARAN[48] has measured the dielectric properties of woods covering a wide range of lignin contents and found that the value of dielec-

tric constant of wood decreases with increasing lignin content. This fact suggests that the dielectric constant of lignin is less than in magnitude than that of cellulose. Since it is reported that there is an excellent linear correlation between the dielectric constant ϵ_l' and the specific gravity γ of lignin[49], the intrinsic dielectric constant of lignin ϵ_l can be calculated from

$$\epsilon_l = \frac{1.34}{\gamma}(\epsilon_l' - 1) + 1, \tag{1.24}$$

where 1.34 is the specific gravity of lignin itself[50]. Table (1.8) shows the calculated values of ϵ_l for three wood MWLs in the absolutely dried condition. The values of the intrinsic dielectric constants of cellulose and lignin will be employed later in the calculation of the dielectric constant of cell wall.

Table 1.8. Intrinsic dielectric constant of MWL.

Species	T(°C)	3 MHz	1 MHz	300 kHz	100 kHz	30 kHz	10 kHz	3 kHz	1 kHz	330 Hz	110 Hz	50 Hz
HINOKI	20	3.90	3.97	4.02	4.07	4.11	4.15	4.19	4.22	4.24	4.26	4.28
BUNA	20	3.81	3.88	3.94	3.97	4.01	4.04	4.05	4.07	4.09	4.12	4.13
HOONOKI	20	3.97	4.04	4.09	4.14	4.18	4.21	4.25	4.28	4.31	4.34	4.35
	0	3.87	3.94	4.00	4.06	4.09	4.13	4.17	4.20	4.23	4.26	4.28
Average	20	3.89	3.96	4.01	4.06	4.10	4.13	4.16	4.19	4.21	4.24	4.25

2. Dielectric properties and structure of wood

If a comparison is made at the same temperature, frequency and moisture content, the order of ϵ' and ϵ'' values is generally L>R≧T as shown in Table (1.1), Figs.(2.1) and (2.2). The purpose of this chapter is to make clear the correlation between the dielectric properties of wood and the wood structure, and to discuss the dielectric anisotropy of wood. Section 2.1 gives an account of the grain angle dependence of the dielectric properties for wood. Sections 2.2 and 2.3 describe the calculations of the dielectric constants of cell wall for late and early woods as well as for ray, and those of wood in the three principal directions. These calculations are based on the models in which the fine structures of cell wall, the proportion and distribution of chemical constitutions, the ratio of cell wall area to cell area, the cell arrangement, and the macroscopic structures such as volumes of late wood and ray, and the annual ring curvature are taken into account. The results obtained will yield valuable informations about the dielectric anisotropy of wood.

2.1 Dielectric properties and grain angle[3,12]

Fig. (2.3) shows the plot of ϵ' against grain angle θ or φ for HOONOKI in LR, LT and TR planes. The value of ϵ' decreases rapidly in LR and LT planes with increase of grain angle, while it increases slightly in TR plane. The ϵ' (θ or

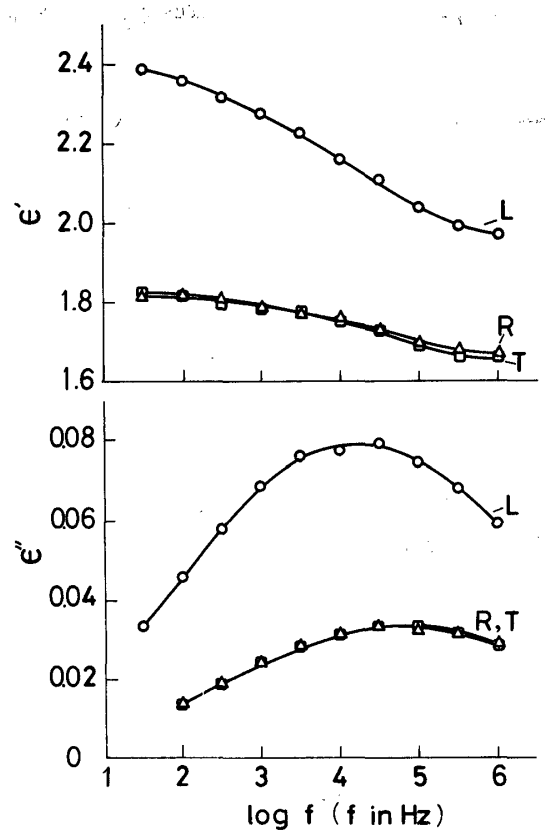

Fig. 2.1. Frequency dependence of ϵ' and ϵ'' for absolutely dried western hemlock in L, R and T directions. (γ= 0,48, T=−58°C).

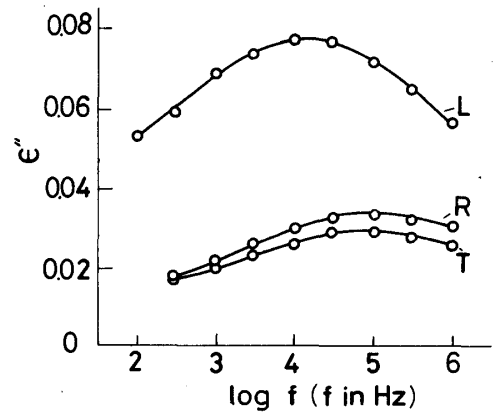

Fig. 2.2. Frequency dependence of ϵ'' for absolutely dried HOONOKI in L, R and T directions. (γ=0.45, T= −58°C).

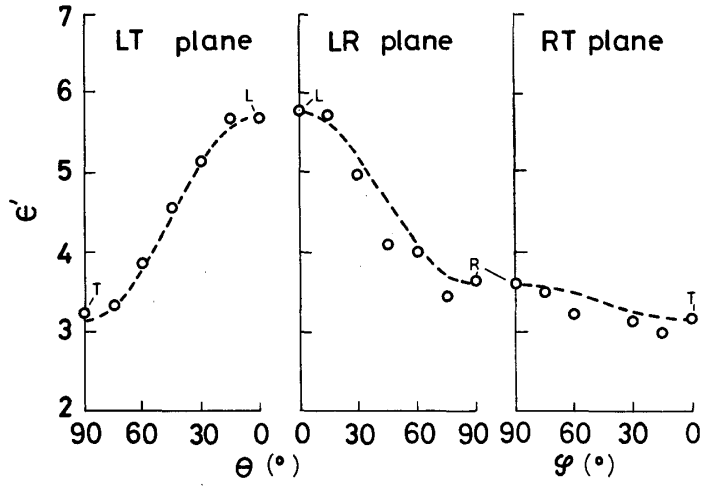

Fig. 2.3. ϵ' versus grain angle curves for HOONOKI. (γ=0.51, m.c.=11.3%, f=10 kHz, T=23°C, dotted lines : Eq. (2.1)).

φ) versus θ or φ curves in the three principal planes can be expressed by the following empirical equation.

$$\epsilon'(x)=\frac{1}{2}\left(|\epsilon'(0)-\epsilon'\left(\frac{\pi}{2}\right)|\cos(2x+x_0)+\epsilon'(0)+\epsilon'\left(\frac{\pi}{2}\right)\right), \tag{2.1}$$

$x=\theta$ or φ

$x_0=0$ in LR and LT planes,

$$\left.\begin{aligned} &x_0=0 \text{ if } \epsilon'(0)\geqq\epsilon'\left(\frac{\pi}{2}\right)\\ &x_0=\pi \text{ if } \epsilon'(0)<\epsilon'\left(\frac{\pi}{2}\right)\end{aligned}\right\} \text{ in TR plane,}$$

where $\epsilon'(0)$ and $\epsilon'(\pi/2)$ are the dielectric constants at θ or $\varphi=0$ and θ or $\varphi=\pi/2$, respectively. The dotted lines in Fig. (2.3) represent the values calculated Eq. (2.1).

As a first approximation, wood may be regarded macroscopically as a mixed body composed of cell wall substance and air in which parallel cylindrical rodlets or square pillars of air are embedded in a cell wall substance. The average diameters of lumen for a tracheid and a vessel are very small as compared with the wave length (10^8 to 3.2 cm) used for the dielectric measurements, so that wood can be regarded as an orthotropic homogeneous dielectric material.

In optical frequency region a mixed body composed of two components with different refractive indices each other shows the structural birefringence[51]. The refractive index $n(\theta)$ for such a body in a given direction is given by[52]

$$\frac{1}{n^2(\theta)}=\frac{\cos^2\theta}{n^2_{/\!/}}+\frac{\sin^2\theta}{n^2_{\perp}}, \tag{2.2}$$

where $n_{/\!/}$ and $n_{\perp}$ are the two principal refractive indices respectively and θ is an

Table 2.1. Values of k calculated for HOONOKI at 20°C.

m.c. (%) / f (Hz) / θ (°)	7.1	0
	3×10^5	1×10^5
0	0.0173	0.0194
5	0.0173	0.0189
10	0.0167	0.0176
15	0.0166	0.0175
20	0.0172	0.0183
25	0.0160	0.0164
30	0.0157	0.0168
45	0.0144	0.0138
60	0.0124	0.0101
65	0.0121	0.0122
70	0.0119	0.0100
90	0.0112	0.0073

angle measured from the principal axis having $n_{//}$. As it is considered that the permiability for a non-magnetic material like wood is unity, so from the MAXWELL's equation the relation between ϵ' or ϵ'' and n are given by

$$\epsilon'(\omega) = n(\omega)^2(1-k(\omega)^2), \tag{2.3}$$

$$\epsilon''(\omega) = 2n(\omega)^2 k(\omega), \tag{2.4}$$

where $k(\omega)$ is the absorption index. The quantities $\epsilon'(\omega)$, $\epsilon''(\omega)$, $n(\omega)$ and $k(\omega)$ are functions of frequency, so these quantities should be compared one another at the same frequency. Thus, from Eqs. (2.3) and (2.4)

$$\frac{1-k(\theta)}{\epsilon'(\theta)} = \frac{(1-k_{//})\cos^2\theta}{\epsilon'_{//}} + \frac{(1-k_{\perp})\sin^2\theta}{\epsilon'_{\perp}}. \tag{2.5}$$

If the dielectric constants in L and R directions, ϵ'_L and ϵ'_R, correspond to $\epsilon'_{//}$ and

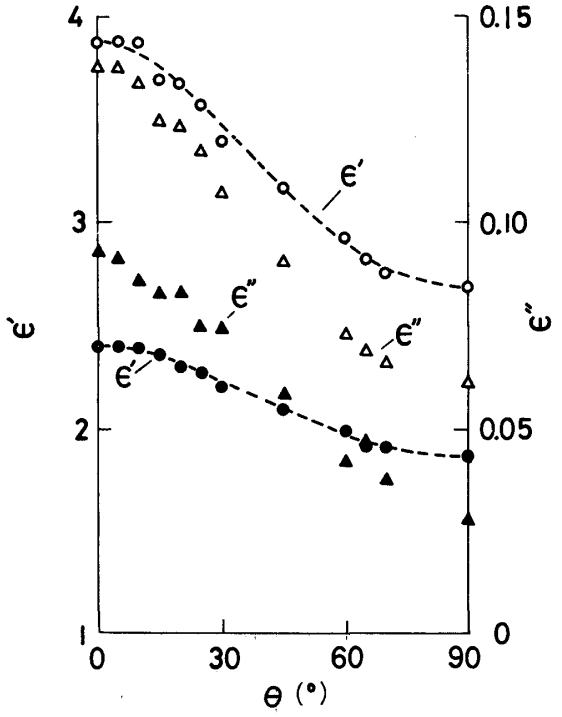

Fig. 2.4. ϵ' and ϵ'' at 20°C for HOONOKI as a function of grain angle in LR plane. (open circles and triangles : m.c.=7.1 % f=300 kHz, closed circles and triangles : m.c.=0 % f=100 kHz, dotted lines : Eq. (2.6)).

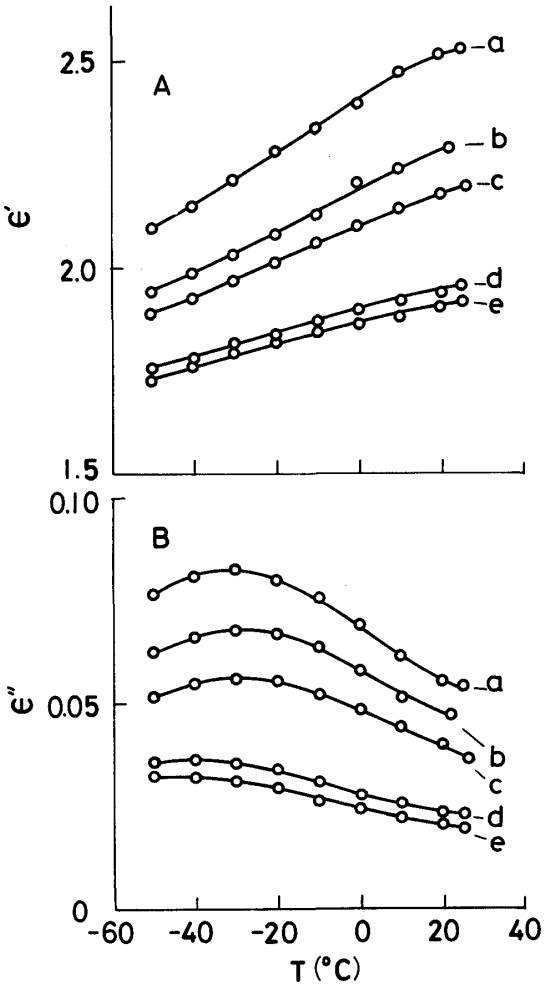

Fig. 2.5. Temperature dependence of ϵ' and ϵ'' at 30 kHz for absolutely dried HOONOKI. (γ=0.50, a : L b : θ=30° c : θ=45° d : θ=70° e : R).

$\epsilon'_{\perp}$ respectively, then the dielectric constant in the direction with a grain angle θ, $\epsilon'(\theta)$, can be calculated from Eq. (2.5). At the two limiting frequencies, f_0 and f_∞, at which dielectric absorptions disappear, $\epsilon''=0$, then $k=0$.

Hence
$$\frac{1}{\epsilon'(\theta)}=\frac{\cos^2\theta}{\epsilon'_L}+\frac{\sin^2\theta}{\epsilon'_R}. \tag{2.6}$$

On the other hand, in the frequency range $f_0<f<f_\infty$, $k\neq 0$. Then, combining Eqs. (2.3) and (2.4) to eliminate n, the absorption index k is written as

$$k=\frac{-\epsilon'+\sqrt{(\epsilon')^2+(\epsilon'')^2}}{\epsilon''}. \tag{2.7}$$

Table (2.1) shows the values of k calculated from Eq. (2.7) for absolutely dried and air dried HOONOKI. As can be seen from this table, the values of k are much less than unity, i.e., $k^2 \ll 1$, and it decreases with increase of θ. Thus, from Eq. (2.3) $\epsilon'(\omega)\approx n(\omega)^2$ in the low moisture content region. In Fig. (2.4) ϵ' and ϵ'' at 100, 300 kHz and 20°C are plotted against θ for HOONOKI containing 0 % and 7.1 % moisture. The dotted lines in the figure show the values calculated from Eq. (2.6) which agree well with the experimental values.

Furthermore, in Fig. (2.5) the ϵ' and ϵ'' versus T curves at various grain angles in LR plane for absolutely dried HOONOKI are shown.

In this connection, putting $x=\sqrt{\epsilon'(\theta)}\sin\theta$, $y=\sqrt{\epsilon'(\theta)}\cos\theta$, and inserting these

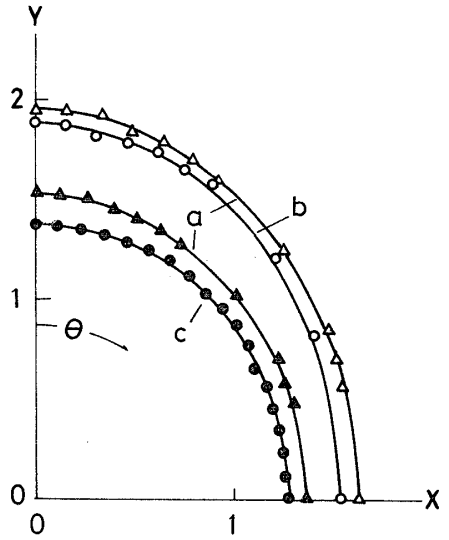

Fig. 2.6. $\sqrt{\epsilon'(\theta)}$ for woods at various grain angles in LR plane. (a : HOONOKI open triangles : m.c.=7.1 % f=300 kHz closed triangles : m.c.=0 % f=100 kHz, b : formosan cypress m.c.=air dry f=1 MHz, c : lawson cypress m.c.=air dry f=9.4 GHz, solid lines : Eq. (2.8)).

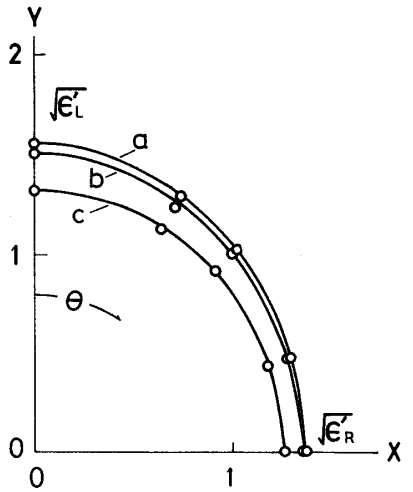

Fig. 2.7. $\sqrt{\epsilon'(\theta)}$ for absolutely dried HOONOKI at various grain angles in LR plane. (a : f=0 Hz, b : f=1 kHz, c : f=∞ Hz, T=−40°C, solid lines : Eq. (2.8)).

into Eq. (2.6), leads to

$$\frac{x^2}{(\sqrt{\epsilon'_R})^2}+\frac{y^2}{(\sqrt{\epsilon'_L})^2}=1. \tag{2.8}$$

This equation represents an elliptic function. The $\sqrt{\epsilon'(\theta)}$ curves at various frequencies for HOONOKI, LOWSON CYPRESS and FORMOSAN CYPRESS calculated from Eq. (2.8) are compared with the experimental values in Figs. (2.6) and (2.7). The values of $\sqrt{\epsilon'(\theta)}$ at the two limiting frequencies are determined from the COLE-COLE plots. As can be seen from these figures, the calculated values agree well with the experimental values in all the cases. Table (2.2) shows the ratio $\sqrt{\epsilon'_L}/\sqrt{\epsilon'_R}$ for absolutely dried HOONOKI which increases with increase of temperature and with decrease of frequency.

Table 2.2. Values of $\sqrt{\epsilon'_L/\epsilon'_R}$ for absolutely dried HOONIKI at various temperatures and frequencies.

f (Hz) / T (°C)	∞	1×10^5	3×10^5	1×10^5	3×10^4	1×10^4	3×10^3	1×10^3	3×10^2	0
20		1.13	1.14	1.14	1.15	1.15	1.16	1.16	1.16	
10		1.12	1.13	1.14	1.14	1.15	1.15	1.15	1.16	
0		1.11	1.12	1.13	1.13	1.14	1.15	1.15	1.15	
−10		1.10	1.11	1.12	1.13	1.13	1.14	1.14	1.14	
−20		1.09	1.10	1.11	1.12	1.13	1.13	1.14	1.14	
−30		1.09	1.10	1.10	1.11	1.12	1.12	1.13	1.14	
−40	1.06	1.08	1.09	1.09	1.10	1.11	1.12	1.12	1.13	1.14
−50	1.05	1.08	1.08	1.09	1.10	1.10	1.11	1.12	1.12	1.14

In general $\epsilon'(\theta,\varphi)$ at a grain angle θ in LR and LT planes and a grain angle φ in TR plane may be expressed by

$$\frac{1}{\epsilon'(\theta,\varphi)}=\frac{\cos^2\theta}{\epsilon'_L}+\frac{\sin^2\theta\cdot\sin^2\varphi}{\epsilon'_R}+\frac{\sin^2\theta\cos\cdot^2\varphi}{\epsilon'_T}, \tag{2.9}$$

where $0°\leqq\theta,\ \varphi\leqq90°$.

2.2 Dielectric constant of cell wall

Cell wall model

Consider now a cell model as shown in Fig. (2.8) in which microfibrils of square cross-section are uniformly distributed in an isotropic matrix. Each microfibril is composed of crystalline and noncrystalline regions in which molecular chains are aligned exactly in the microfibril direction(1-direction), and they make an angle θ with the direction of cell axis (L direction). Furtheremore, assume that the dielectric constants of crystalline and noncrystalline materials for a microfibril, ϵ_C and ϵ_A, are given by

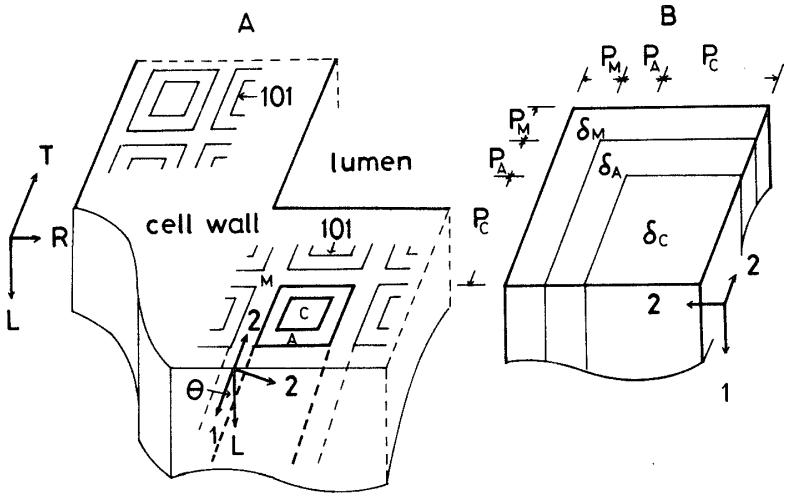

Fig. 2.8. A: Cell wall model. (101) plane lies parallel to lumen side. (θ: average microfibril angle, C: crystalline region, A: noncrystalline region, M: matrix), B: Unit cell wall model. (δ: volume fraction, P: length fraction).

$$\epsilon_{C1}=\epsilon_{\infty 1},$$
$$\epsilon_{A1}=\epsilon_{\infty 1}\psi_1,$$
$$\epsilon_{C2}=\epsilon_{\infty 1}-(n_1^2-n_2^2),$$
$$\epsilon_{A2}=\epsilon_{C2}\left\{\frac{\psi_1\epsilon_{C1}-(n_1^2-n_2^2)}{\epsilon_{C1}-(n_1^2-n_2^2)}\right\}, \tag{2.10}$$

where the subscripts 1 and 2 implies the directions parallel and perpendicular to microfibrils respectively, the subscripts C and A implies the crystalline and noncrystalline regions respectively, and ϵ_∞ and n^2 are the dielectric constants at frequencies in infra-red and optical regions respectively. Then, the dielectric constants of cell wall in the 1- and 2-directions, ϵ_{Cw1} and ϵ_{Cw2}, are given by

$$\epsilon_{Cw1}=P_C^2\epsilon_{C1}+\{(P_A+P_C)^2-P_C^2\}\epsilon_{A1}+\{1-(P_A+P_C)^2\}\epsilon_M, \tag{2.11}$$
$$\epsilon_{Cw2}=\{1-(P_A+P_C)\}\epsilon_M+P_A\epsilon_x+P_C\epsilon_y, \tag{2.12}$$

where
$$\frac{1}{\epsilon_x}=\frac{P_A+P_C}{\epsilon_{A2}}+\frac{P_M}{\epsilon_M},$$
$$\frac{1}{\epsilon_y}=\frac{P_A}{\epsilon_{A2}}+\frac{P_C}{\epsilon_{C2}}+\frac{P_M}{\epsilon_M},$$
$$P_C+P_A+P_M=1,$$

ϵ_M is the dielectric constant of matrix substance, P_C, P_A and P_M are the length fractions of crystalline region, noncrystalline region and matrix as shown in Fig. (2.8b) respectively. Therefore, the dielectric constant of cell wall in the direction Θ, $\epsilon_{Cw}(\Theta)$, is given by

$$\frac{1}{\epsilon_{Cw}(\Theta)}=\frac{\cos^2\Theta}{\epsilon_{Cw1}}+\frac{\sin^2\Theta}{\epsilon_{Cw2}}. \tag{2.13}$$

If $\Theta=\theta$, where θ is the average microfibril angle in wood, $\epsilon_{Cw}(\theta)$ and $\epsilon_{Cw}(90-\theta)$ give

the dielectric constants of cell wall in L and R or T directions of wood respectively.

The intrinsic dielectric constant of cellulose parallel to fiber axis at frequencies in infra-red region, $\epsilon_{C\infty}(\theta_C)$, is written as

$$\frac{1}{\epsilon_{C\infty}(\theta_C)}=\frac{\cos^2\theta_C}{\epsilon_{C1}}+\frac{\sin^2\theta_C}{\epsilon_{C2}}. \tag{2.14}$$

The ϵ_{C1} value at 20°C calculated from Eq. (2.14) by putting $\theta_C=30°$ and $\epsilon_{C\infty}(\theta_C)=4.10$ (see Table 1.7) is 4.17.

On the other hand, the dielectric constants in the 1-, 2- and θ-directions for cellulose microfibril having a crystallinity ϕ, ϵ_{Cf1}, ϵ_{Cf2} and $\epsilon_{Cf}(\theta_C)$, are given by

$$\epsilon_{Cf1}=(1-\phi)\epsilon_{A1}+\phi\epsilon_{C1} \tag{2.15}$$

$$\epsilon_{Cf2}=(1-\sqrt{\phi})\epsilon_{A2}+\sqrt{\phi}\,\epsilon_x, \tag{2.16}$$

$$\frac{1}{\epsilon_{Cf}(\theta_C)}=\frac{\cos^2\theta_C}{\epsilon_{Cf1}}+\frac{\sin^2\theta_C}{\epsilon_{Cf2}} \tag{2.17}$$

$$\frac{1}{\epsilon_x}=\frac{1-\sqrt{\phi}}{\psi_1\epsilon_{C1}-(n_1^2-n_2^2)}+\frac{\sqrt{\phi}}{\epsilon_{C1}-(n_1^2-n_2^2)},$$

where $\epsilon_{Cf}(\theta_C)$: (see Table (1.7)), $\epsilon_{C1}=4.17$ (at 20°C), $\phi=0.68$, $n_1=1.618$, $n_2=1.543$, $\theta_C=30°$. From Eqs. (2.10) and (2.15) through (2.17), ψ_1, i.e., the ratio of ϵ_{A1} to ϵ_{C1}, can be calculated. The ψ_1 values calculated in this manner at various frequencies are listed in Table (2.3).

Table 2.3. Values of ψ_1 at 20°C.

f (kHz)	3×10^3	1×10^3	3×10^2	1×10^2	3×10	1×10	3	1	3.3×10^{-1}
ψ_1	1.44	2.03	2.55	2.90	(3.16)*	(3.34)	(3.47)	(3.61)	(3.69)

* In the frequency range higher than 30 kHz an additional dispersion, probably due to the interfacial polarization, may be included.

Dielectric constants of matrix and cell wall

We shall now calculate ϵ_M value for the four cases. Matrix model I (in which spherical pentosan molecules are uniformly embedded in lignin.)

$$\epsilon_l\epsilon_M^3-3\epsilon_P\epsilon_l\epsilon_M^2+\left\{\left(\frac{\delta_l}{\delta_l+\delta_P}\right)^3(\epsilon_P-\epsilon_l)^3+3\epsilon_P^2\epsilon_l\right\}\epsilon_M-\epsilon_P^3\epsilon_l=0, \tag{2.18}$$

$$\epsilon_P=\frac{1}{3}\left[\epsilon_{C1}+2\left\{\epsilon_{C1}-(n_1^2-n_2^2)\right\}\right], \tag{2.19}$$

$$P_C=\sqrt{\delta_C\phi},\quad P_A=\sqrt{\delta_C+\delta_m}-P_C,\quad \delta_l+\delta_P+\delta_m+\delta_C=1,$$

where ϵ_P and ϵ_l are the dielectric constants of pentosan and lignin respectively, and δ_C and ϕ are the volume fraction and the crystallinity for cellulose respectively, and δ_l, δ_P and δ_m are the volume fractions of lignin, pentosan and mannan respectively. Matrix model II (in which spherical mannan molecules are uniformly embedded in lignin.)

$$\epsilon_l\epsilon_M{}^3-3\epsilon_m\epsilon_l\epsilon_M{}^2+\left\{\left(\frac{\delta_l}{\delta_l+\delta_m}\right)^3(\epsilon_m-\epsilon_l)^3+3\epsilon_m{}^2\epsilon_l\right\}\epsilon_M-\epsilon_m{}^3\epsilon_l=0, \quad (2.20)$$

$$\epsilon_m=\frac{1}{3}\left[\epsilon_{C1}\psi_1+2\epsilon_{C2}\left\{\frac{\psi_1\epsilon_{C1}-(n_1{}^2-n_2{}^2)}{\epsilon_{C1}-(n_1{}^2-n_2{}^2)}\right\}\right], \quad (2.21)$$

$$P_A=\sqrt{\delta_C+\delta_P}-P_C,\quad P_C=\sqrt{\delta_C\phi+\delta_P},$$

where ϵ_m is the dielectric constant of mannan. Matrix model III (in which spherical-spherical mixtures of mannan and pentosan are uniformly embedded in lignin.)

$$\epsilon_l\epsilon_M{}^3-3\epsilon_{mP}\epsilon_l\epsilon_M{}^2+\left\{\left(\frac{\delta_l}{\delta_l+\delta_P+\delta_m}\right)^3(\epsilon_{mP}-\epsilon_l)^3+3\epsilon^2{}_{mP}\epsilon_l\right\}\epsilon_M-\epsilon^3{}_{mP}\epsilon_l=0, \quad (2.22)$$

$$\epsilon_{mP}=\frac{1}{4}(2\epsilon_a-\epsilon_b+\sqrt{(2\epsilon_a-\epsilon_b)^2+8\epsilon_P\epsilon_m}), \quad (2.23)$$

$$\epsilon_a=\frac{\epsilon_P\delta_P}{\delta_P+\delta_m}+\frac{\epsilon_m\delta_m}{\delta_P+\delta_m},\quad \epsilon_b=\frac{\epsilon_P\delta_m}{\delta_P+\delta_m}+\frac{\epsilon_m\delta_P}{\delta_P+\delta_m},$$

$$P_A=\sqrt{\delta_C}-P_C,\quad P_C=\sqrt{\delta_C\phi},$$

where ϵ_{mP} is the dielectric constant of mannan-pentosan mixture (spherical-spherical mixture[55]). Matrix model IV (composed of lignin.)

$$\epsilon_M=\epsilon_l,\quad P_A=\sqrt{\delta_C+\delta_P+\delta_m}-P_C,\quad P_C=\sqrt{\delta_C\phi+\delta_P}.$$

In Table (2.4) the ϵ_M values at 20°C and 1 MHz calculated using the constants

Table 2.4. Values of ϵ_M for tracheids in early and late woods as well as for ray.

Model	I	II	III	IV
Early wood	3.97	4.88	4.78	3.96
Late wood	3.97	4.92	4.80	3.96
Ray	3.97	4.49	4.41	3.96

Table 2.5. Constants.

n_1	n_2	ϕ	ϵ_{c1}	ϵ_l	ψ_1
1.618	1.543	0.68	4.17	3.96	2.03

Table 2.6. Volume fractions of chemical constituents for tracheids in early and late woods as well as for ray.

	δ_c	δ_m	δ_p	δ_l
Early wood	0.474	0.123	0.059	0.334
Late wood	0.519	0.115	0.064	0.302
Ray	0.319	0.088	0.127	0.467

These values are calculated from specific gravities ($\gamma_c=1.53$, $\gamma_m=1.50$, $\gamma_p=1.50$, $\gamma_l=1.34$) and weight fractions of chemical constituents.

shown in Tables (2.5) and (2.6) for tracheides in early and late woods as well as for ray are listed. It has been reported that mannan is closely associated with cellulose in microfibrils but xylan appears to be located within the interstices and upon the surfaces of microfibrils since the width of the (002) X-ray diffraction peak narrows as mannan-rich hemicelluloses are extracted and xylan removal does not produce this effect[56]. Hence, the ϵ_M value for the model I will be used hereafter.

Fig. (2.9) shows the dielectric constants of cell wall in the directions parallel and perpendicular to microfibrils, ϵ_{Cw1} and ϵ_{Cw2}, versus log f curves for tracheides in early and late woods as well as for ray. Using the average microfibril angles for a few coniferous woods listed in Table (2.7)[57] the dielectric constants of radial and tangential cell wall in L, R and T directions can be calculated from Eq.(2.13). In Table (2.8) these values calculated are shown.

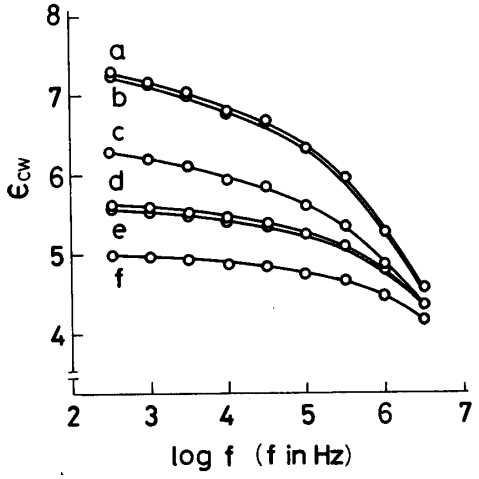

Fig. 2.9. Frequency dependence of the calculated dielectric constants of cell wall in the directions parallel and perpendicular to microfibrils for tracheids in early and late woods and for ray. (T=20°C, m.c.=0%, a : late wood 1-direction b : early wood 1-direction c : ray 1-direction d : late wood 2-direction e : early wood 2-direction f : ray 2-direction).

Table 2.7. Average microfibril angles for four coniferous woods.

(Degree)	Early wood		Late wood	
Species	Radial wall	Tangential wall	Radial wall	Tangential wall
ICHII	23.5	22.0	12.9	19.7
HINOKI	35.6	12.5	4.2	8.5
KOOYAMAKI	32.5	28.5	7.3	10.8
KONOTEGASHIWA	28.2	26.2	14.2	—
Average	30.0	22.3	9.7	13.0

Average microfibril angle of ray : 45.0° (calculated value).

Table 2.8. Dielectric constants of radial and tangential cell walls in L, R and T directions.

	Early wood		Late wood		Ray
	Radial wall	Tangential wall	Radial wall	Tangential wall	
L	5.09	5.14	5.23	5.22	4.64 (4.46)*
R	4.84	4.73	4.77	4.76	4.64
T	4.73	4.80	4.76	4.78	4.64 (4.64)*

* Direction of cell wall thickness.

2.3 Dielectric constant of wood

In this section, by using the ϵ_{Cw} values calculated in the preceding section and by considering the ratio of cell wall area to cell area, i.e., the cell wall fraction, and the cell arrangement, let us evaluate the dielectric constants for early and late woods as well as for ray cell and those for wood in the three principal directions, and discuss the dielectric anisotropy in wood in the transverse directions.

Dielectric constants of early and late woods[53,54]

The cell aggregation in cross section of coniferous wood may be represented by a model illustrated in Fig. (2.10). In this model R_0 and T_0 are the radial and tangential diameters of cell, L_R and L_T are the radial and tangential diameters of lumen, $M_{R\text{ or }T}$ and $\theta_{R\text{ or }T}$ are the thickness and the average microfibril angle in

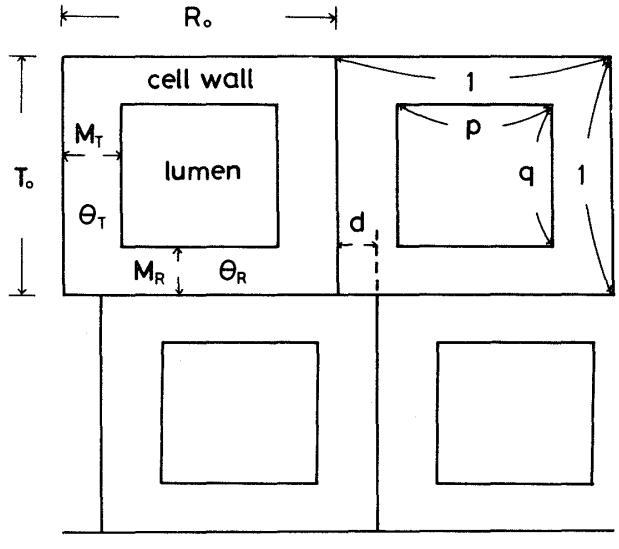

Fig. 2.10. Model of coniferous wood (cross section). (T_O=tangential diameter, R_O=radical diameter, M_T=thickness of tangential wall, M_R=thickness of radial wall, θ_T : average microfibril angle in trangential wall, θ_R : average microfibril angle in radial wall, $p=(R_O-M_T)/R_O$, $q=(T_O-M_R)/T_O$, d : a parameter indicating irregular arrangement of cells).

radial or tangential wall, and $p=L_R/R_0$ and $q=L_T/T_0$. In this case the dielectric constant of a cell in L direction ϵ_{ll} is given by

$$\epsilon_{ll}=\frac{W\{\epsilon_{Cw}(\theta_R)+\epsilon_{Cw}(\theta_T)\}}{2}+(1-W)\epsilon_a, \tag{2.24}$$

where W is the ratio of cell wall area to cell area in cross section, and $\epsilon_{Cw}(\theta_R)$ and $\epsilon_{Cw}(\theta_T)$ are the dielectric constants in L direction for radial and tangential cell walls respectively, and ϵ_a ($=1.00$) is the dielectric constant of air. Here, the quantity $\epsilon_{Cw}(\theta_{R\text{ or }T})$ can be calculated from Eq. (2.13). The dielctric constant in R direction for the model ϵ_{rr} is given by

$$\epsilon_{rr}=(1-q)\epsilon_{r1}+q\epsilon_{r2}, \tag{2.24}$$

where

$$\frac{1}{\epsilon_{r1}}=\frac{1}{2}\left\{\frac{1+p}{\epsilon_{Cw}(90-\theta_R)}+\frac{1-p}{\epsilon_{Cw2}}\right\},$$

$$\frac{1}{\epsilon_{r2}}=\frac{1-p}{\epsilon_{Cw2}}+\frac{p}{\epsilon_a}.$$

On the other hand, the dielectric constant in T direction for the model is given by

when $0\leqq p\leqq\frac{1}{2}$,

if $0\leqq d\leqq p$, $\epsilon_{tt}=(1-p-d)\epsilon_{t1}+2d\epsilon_{t2}+(p-d)\epsilon_{t3}$, (2.26)

if $p\leqq d\leqq\frac{1}{2}$, $\epsilon_{tt}=(1-2p)\epsilon_{t1}+2p\epsilon_{t2}$, (2.27)

where $\frac{1}{2}\leqq p\leqq 1$,

if $0\leqq d\leqq 1-p$, $\epsilon_{tt}=(1-p-d)\epsilon_{t1}+2d\epsilon_{t2}+(p-d)\epsilon_{t3}$, (2.28)

if $1-p\leqq d\leqq\frac{1}{2}$, $\epsilon_{tt}=2(1-p)\epsilon_{t2}+(2p-1)\epsilon_{t3}$, (2.29)

where

$$\frac{1}{\epsilon_{t1}}=\frac{1}{2}\left\{\frac{1+q}{\epsilon_{Cw}(90-\theta_T)}+\frac{1-q}{\epsilon_{Cw2}}\right\},$$

$$\frac{1}{\epsilon_{t2}}=\frac{1+q}{4\epsilon_{Cw}(90-\theta_T)}+\frac{3(1-q)}{4\epsilon_{Cw2}}+\frac{q}{2\epsilon_a},$$

$$\frac{1}{\epsilon_{t3}}=\frac{1-q}{\epsilon_{Cw2}}+\frac{q}{\epsilon_a}.$$

In the case of $\theta_R=\theta_T$ and $d=0$, $\epsilon_{rr}-\epsilon_{tt}=(p-q)f(p,q)$, where $f(p,q)$ is a function of p and q. If the value of ϵ_{Cw} is of the order shown in Fig. (2.9), then $f(p,q)>0$. Thus, if $p\gtrless q$, $\epsilon_{rr}\gtrless\epsilon_{tt}$. Putting $x=L_R/2M_T$, $y=R_0/T_0$, $z=M_T/M_R$ and $y'=y/z$, then $p=x/(x+1)$ and $q=1-y'/(x+1)$. As $W=1-pq$, x is written as[58]

$$x=\frac{1+y'-2W+\sqrt{(1+y'-2W)^2+4W(1-W)}}{2W} \tag{2.30}$$

Table (2.9) shows the calculated values of x, p and q. As $p>q$ in early wood, so $\epsilon_{rr}>\epsilon_{tt}$. On the other hand, as $p<q$ in late wood, so $\epsilon_{rr}<\epsilon_{tt}$. In the case of $\theta_R\gtrless\theta_T$, $\epsilon_{rr}(\theta_R\gtrless\theta_T)\gtrless\epsilon_{rr}(\theta_R=\theta_T)$, while $\epsilon_{rr}(\theta_R\gtrless\theta_T)\lesseqgtr\epsilon_{rr}(\theta_R=\theta_T)$. According to Onaka $\theta_R>\theta_T$ in early wood and $\theta_R<\theta_T$ in late wood as shown in Table (2.7)[57]. Then, $\epsilon_{rr}>$

Table 2.9. Values of x, p and q.

	Early wood	Late wood
W*	0.31	0.79
y*	1.24	0.58
z*	1.02	0.75
x	5.56	0.65
p	0.85	0.39
q	0.81	0.53

* Average value of five coniferous woods (After SUZUKI[60] and SAIKI[50]).

ϵ_{tt} in early wood and $\epsilon_{rr}<\epsilon_{tt}$ in late wood. In the same manner, the dielectric constants in L and the transverse directions of wood for ray cell in early and late wood portions, $\epsilon_{L\,ray\,f}$, $\epsilon_{L\,ray\,s}$, $\epsilon_{\perp\,ray\,f}$ and $\epsilon_{\perp\,ray\,s}$, can be calculated.

Dielectric anisotropy in wood

Let us consider wood as a composite material shown in Fig. (2.11) which is composed of early and late wood tracheids and ray cells. Then, the dielectric constants in the three principal directions for such a model, ϵ_L, ϵ_T and ϵ'_R, can be calculated by

$$\epsilon_L=\delta_r\{\delta_s\epsilon_{\perp\,ray\,s}+(1-\delta_s)\epsilon_{\perp\,ray\,f}\}+(1-\delta_r)\{\delta_s\epsilon_{lls}+(1-\delta_s)\epsilon_{llf}\}, \quad (2.31)$$

$$\epsilon_T=\frac{\delta_r}{\delta_s\epsilon_{\perp\,ray\,s}+(1-\delta_s)\epsilon_{\perp\,ray\,f}}+\frac{1-\delta_r}{\delta_s\epsilon_{tts}+(1-\delta_s)\epsilon_{ttf}}, \quad (2.32)$$

$$\epsilon'_R=\delta_r\left\{\frac{\delta_s}{\epsilon_{L\,ray\,s}}+\frac{1-\delta_s}{\epsilon_{L\,ray\,f}}\right\}^{-1}+(1-\delta_r)\left\{\frac{\delta_s}{\epsilon_{rrs}}+\frac{1-\delta_s}{\epsilon_{rrf}}\right\}^{-1},$$

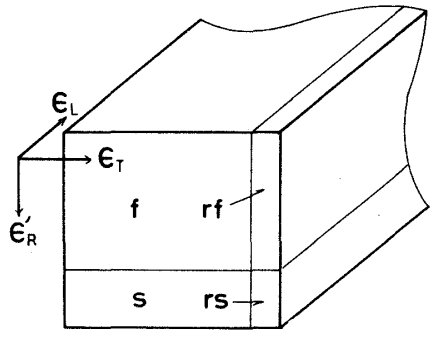

Fig. 2.11. Wood model composed of early and late wood tracheids and ray cells. (f : early wood tracheids, s : late wood tracheids, rf : ray cells in early wood portion, rs : ray cells in late wood portions).

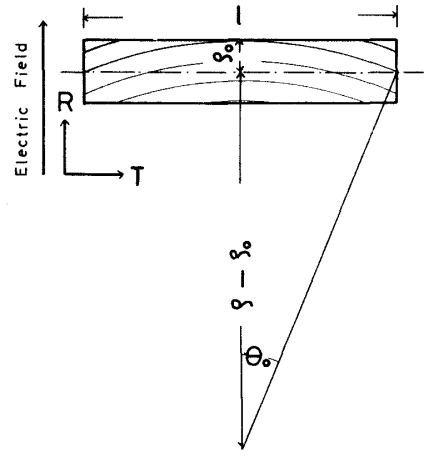

Fig. 2.12. Model of wood sample used for the measurement of the dielectric constant of wood in R direction.

where δ_r is the ray cells fraction, i.e., the proportional volume of ray parenchyma cells, δ_s is the late wood fraction, and the subscripts f and s implies early and late woods respectively. Considering the curvature of annual ring (see Fig. (2.12)) the

Table 2.10. Values of dielectric constants for wood in L, R and T directions.

δ_s	γ	ϵ_L	d=0		d=0.05		d=0.10		d=0.15	
			ϵ_R	ϵ_T	ϵ_R	ϵ_T	ϵ_R	ϵ_T	ϵ_R	ϵ_T
0.0	0.45	2.25	1.84	1.72	1.83	1.62	1.82	1.51	1.82	1.41
0.1	0.52	2.45	1.92	1.90	1.92	1.81	1.92	1.71	1.91	1.62
0.2	0.59	2.66	2.02	2.08	2.02	2.00	2.01	1.91	2.01	1.83
0.3	0.66	2.86	2.12	2.26	2.12	2.19	2.12	2.11	2.12	2.04
0.4	0.73	3.06	2.24	2.44	2.24	2.37	2.23	2.31	2.23	2.25
0.5	0.80	3.27	2.37	2.61	2.36	2.56	2.36	2.51	2.36	2.46
0.6	0.87	3.47	2.51	2.79	2.51	2.75	2.51	2.71	2.50	2.67
0.7	0.94	3.67	2.67	2.97	2.67	2.94	2.66	2.91	2.66	2.88
0.8	1.01	3.88	2.85	3.15	2.85	3.13	2.84	3.11	2.84	3.09
0.9	1.08	4.08	3.05	3.33	3.05	3.32	3.05	3.31	3.05	3.30
1.0	1.15	4.29	3.29	3.50	3.29	3.50	3.29	3.50	3.29	3.50

δ_s : fraction of late wood, γ : specific gravity, d : parameter indicating irregular arrangement of cells.

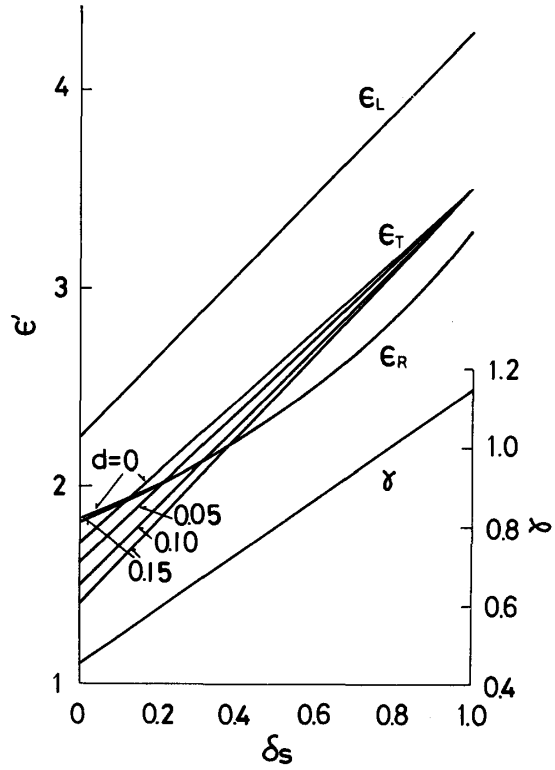

Fig. 2.13. Late wood fraction dependence of the calculated dielectric constants of wood in L, R and T directions. (f=1 MHz, T=20°C).

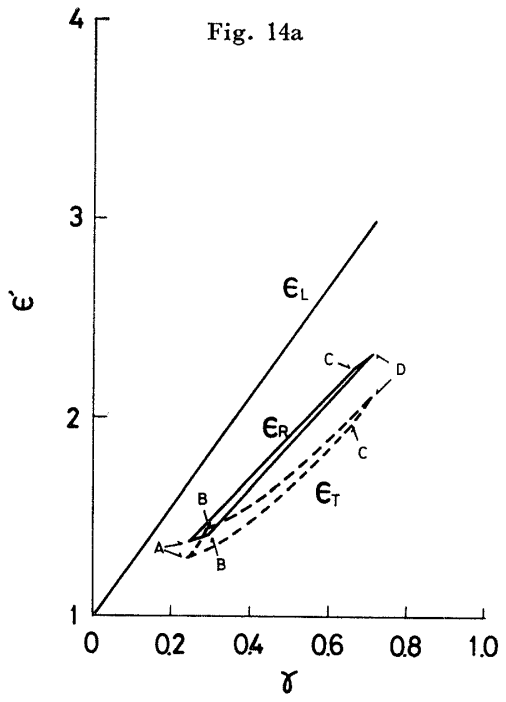

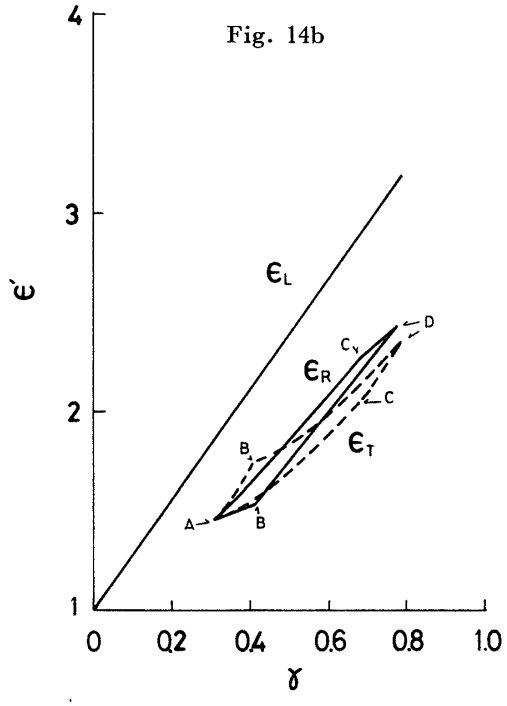

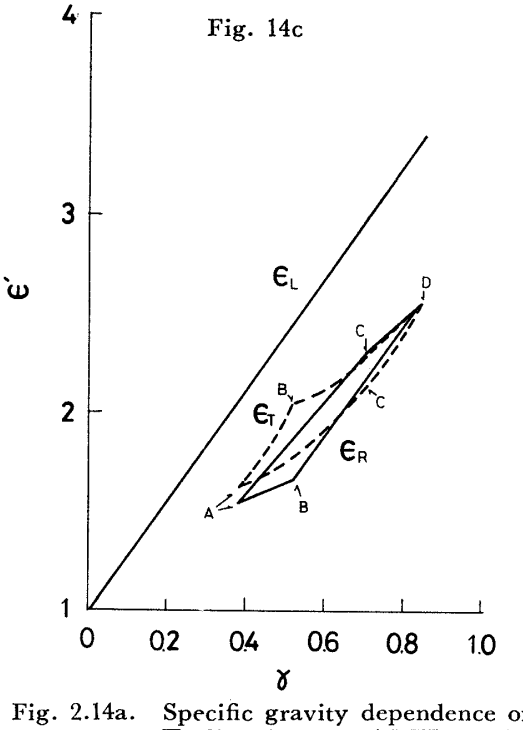

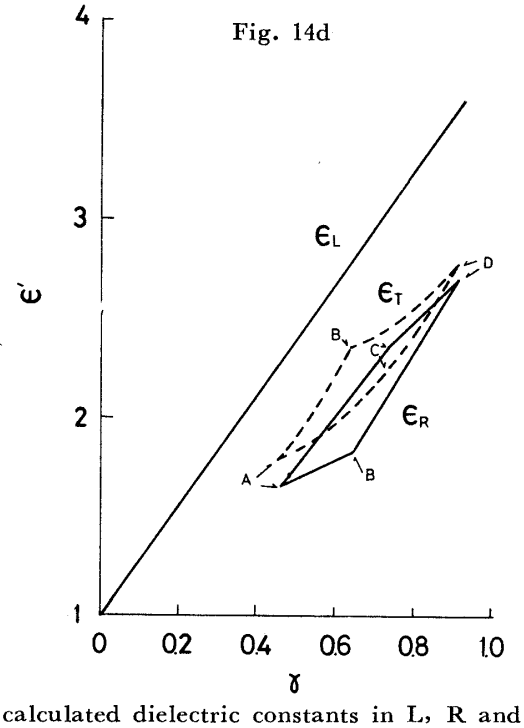

Fig. 2.14a. Specific gravity dependence of the calculated dielectric constants in L, R and T directions at 1 MHz and 20°C. (d=0.10, δ_s=0.1, δ_r=0.05, AB : W_f=0.12 W_s=0.60 to 0.92, CD : W_f=0.44 W_s=0.60 to 0.92, AC : W_s=0.60 W_f=0.12 to 0.44, BD : W_s=0.92 W_f=0.12 to 0.44).

Fig. 2.14b. Specific gravity dependence of the calculated dielectric constants in L, R and T directions at 1 MHz and 20°C. (d=0.10, δ_s=0.2).

Fig. 2.14c. Specific gravity dependence of the calculated dielectric constants in L, R and T directions at 1 MHz and 20°C. (d=0.10, δ_s=0.3).

Fig. 2.14d. Specific gravity dependence of the calculated dielectric constants in L, R and T directions at 1 MHz and 20°C. (d=0.10, δ_s=0.4).

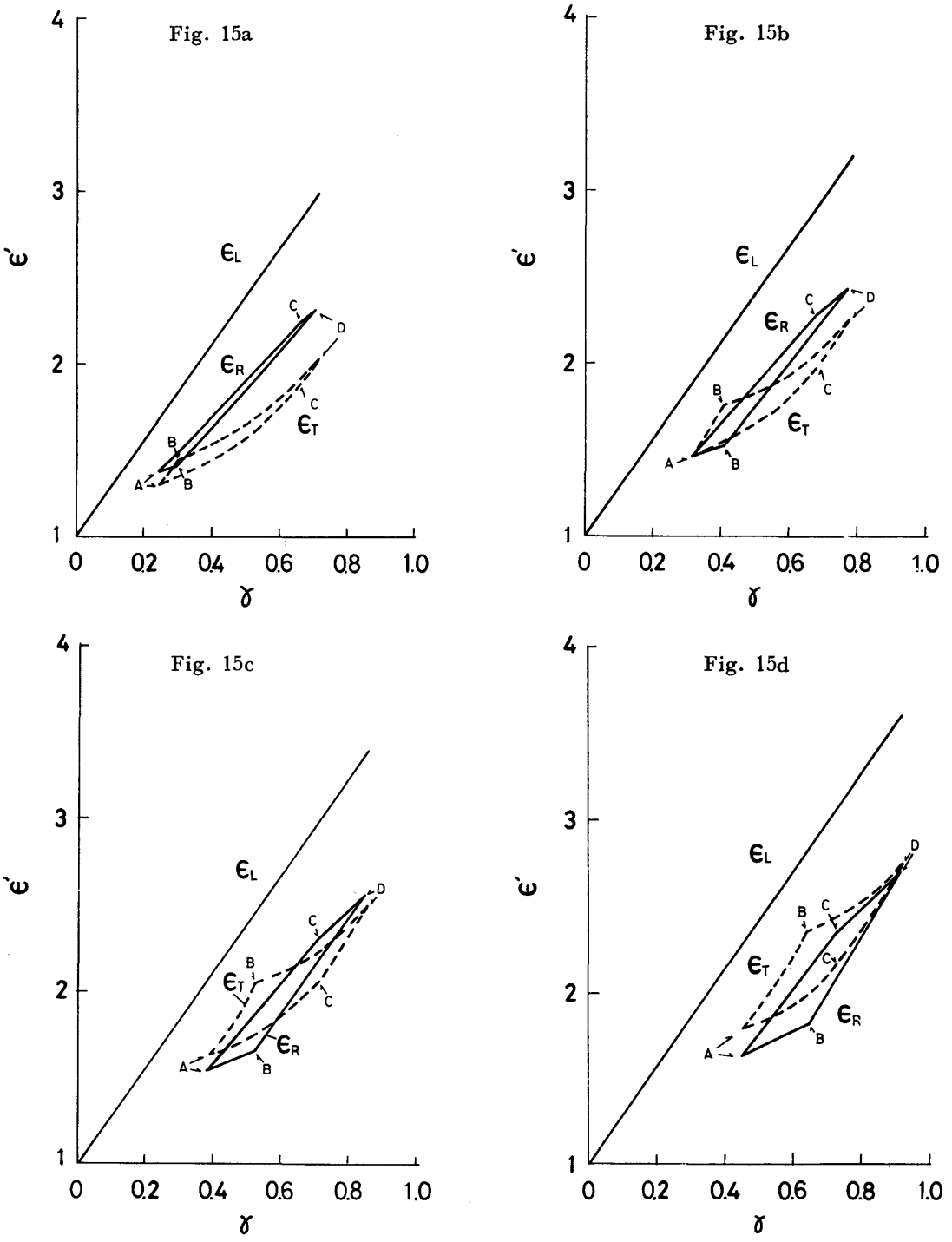

Fig. 2.15a. Specific gravity dependence of the calculated dielectric constants in L, R and T directions at 1 MHz and 20°C. (d=0.15, δ_s=0.1, δ_r=0.05, AB : W_f=0.12 W_s=0.60 to 0.92, CD : W_f=0.44 W_s=0.60 to 0.92, AC : W_s=0.60 W_f=0.12 to 0.44, BD : W_s=0.92 W_f=0.12 to 0.44).

Fig. 2.15b. Specific gravity dependence of the calculated dielectric constants in L, R and T directions at 1 MHz and 20°C. (d=0.15, δ_s=0.2).

Fig. 2.15c. Specific gravity dependence of the calculated dielectric ocnstants in L, R and T directions at 1 MHz and 20°C. (d=0.15, δ_s=0.3).

Fig. 2.15d. Specific gravity dependence of the calculated dielectric constants in L, R and T directions at 1 MHz and 20°C. (d=0.15, δ_s=0.4).

dielectric constant in R direction is given by

$$\epsilon_R = \frac{1}{\theta_0}\int_0^{\theta_0} \epsilon(\theta)\,d(\theta) = \frac{1}{\theta_0}\sqrt{\epsilon'_R \epsilon_T}\,\tan^{-1}\left(\sqrt{\frac{\epsilon'_R}{\epsilon_T}}\tan\theta_0\right), \qquad (2.33)$$

where $$\frac{1}{\epsilon(\theta)} = \frac{\cos^2\theta}{\epsilon'_R} + \frac{\sin^2\theta}{\epsilon_T}, \quad \theta_0 = \sin^{-1}\left(\frac{4\rho_0}{l}\right).$$

Table (2.10) shows the values of ϵ_L, ϵ_R and ϵ_T calculated from Eqs. (2.31) through (2.33) by putting $\delta_r = 0.05$, d = 0, 0.05, 0.10, 0.15, $\delta_s = 0.0$ to 1.0, and by using the values shown in Table (2.9). Furthermore, in Fig. (2.13) the dielectric constants in the three principal directions at each d value as a function of late wood fraction are shown. The values of ϵ_L and ϵ_T increase linearly with δ_s but those of ϵ_R increase curvelinearly. The dielectric constant is almost independent of d in L and R directions but depends very markedly on d in T direction. The intersection point of the ϵ_R and ϵ_T versus δ_s curves moves to higher δ_s value with increase of d. In Figs. (2.14) and (2.15) the theoretical dielectric constant curves in the three

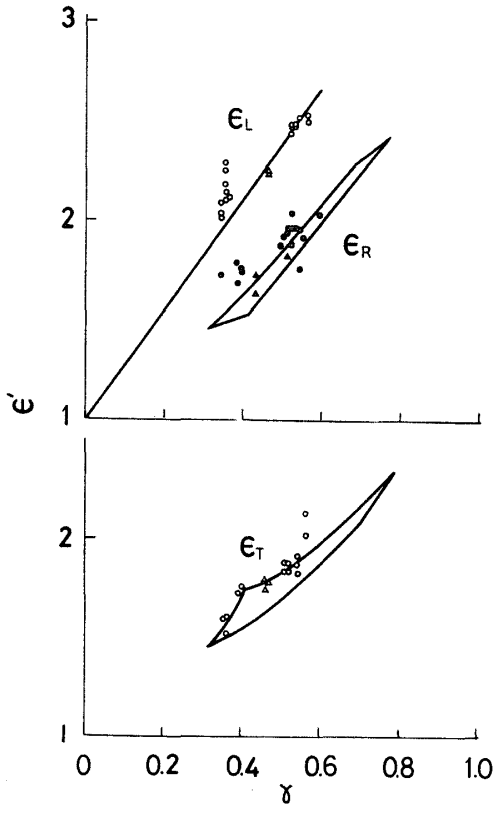

Fig. 2.16. Specific gravity dependence of ϵ' at 1 MHz for absolutely dried wood. (solid lines : calculated values d=0.10 δ_s=0.2 δ_f=0.05, circles : HINOKI triangles : AKAMATSU (experimental values)).

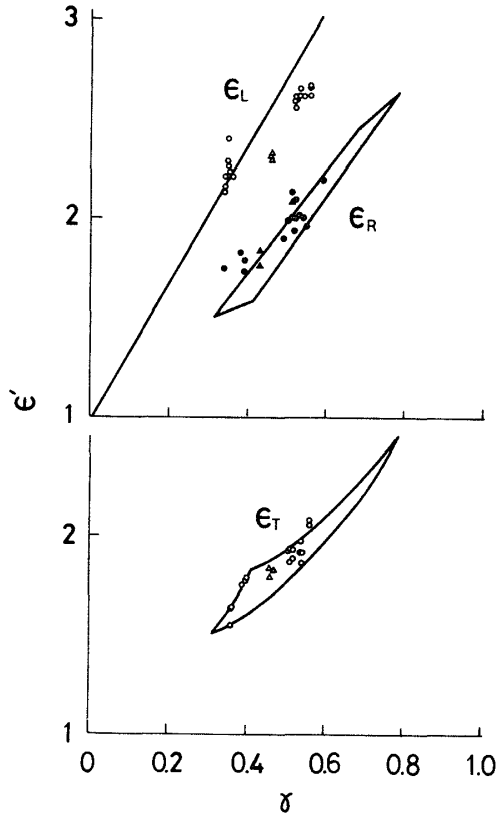

Fig. 2.17. Specific gravity dependence of ϵ' at 100 kHz for absolutely dried wood. (solid lines : calculated values d=0.10 δ_s=0.2 δ_f=0.05, circles : HINOKI triangles : AKAMATSU (experimental values)).

principal directions at 1 MHz and 20°C as a function of specific gravity are shown. In these figures the curves AB and CD represent the constant W_f dielectric constant curves (AB: $W_f=0.12$, CD: $W_f=0.44$, $W_s=0.60$ to 0.92), and the curves AC and BD represent the constant W_s dielectric constant curves (AC:$W_s=0.60$, BD: $W_s=0.92$, $W_f=0.12$ to 0.44). In Figs. (2.16) and (2.17) the theoretical dielectric constant values at 1 MHz and 100 kHz and at 20°C ($d=0.10$, $\delta_s=0.2$, $\delta_r=0.05$) are made a comparison with the experimental values.

From these results it is considered that the anisotropy of dielectric constant in the transverse directions depends on the average microfibril angle, the late wood fraction, the cell form (p and q), the curvature of annual ring, the cell wall fraction, the cell arrangement (d) and so on, and above all it is remarkably influenced by both the late wood fraction and the cell arrangement.

Acknowledgement

The author would like to acknowledge the continuing guidance and encouragement of Professor Dr. T. YAMADA. The author also wishes to thank Professor Dr. T. HIGUCHI for his helpful advice and Mr. T. TANAKA for his collaboration. This research was supported in part by a Scientific Research Fund of the Ministry of Education.

References

1) H. FRÖLICH, Theory of DIELECTRICS, Claredon Press, Oxford, (1958).
2) K. S. COLE and R. H. COLE, J. Chem. Phys., **9**, 341 (1941).
3) T. TANAKA, M. NORIMOTO and T. YAMADA, Mokuzai Gakkaishi, **21**, 129 (1975).
4) M. NORIMOTO and T. YAMADA, Wood Research, No. 51, 12 (1971).
5) A. J. NANASSY, Wood Sci. Techn., **4**, 104 (1970).
6) R. FUOSS and J. G. KIRKWOOD, J. Am. Chem. Soc., **63**, 385 (1941).
7) M. NORIMOTO and T. YAMADA, Mokuzai Gakkaishi, **21**, (1975) in press.
8) J. G. FERRY, Viscoelestic Properties of Polymer, John Wiley & Sons, New York-London, (1961).
9) M. NORIMOTO and T. YAMADA, Wood Research, No. 46, 1 (1969).
10) M. NORIMOTO and T. YAMADA, ibid, No. 50, 36 (1970).
11) M. NORIMOTO and T. YAMADA, Mokuzai Gakkaishi, **16**, 364 (1970).
12) M. NORIMOTO and T. YAMADA, Wood Research, No. 52, 31 (1972).
13) W. KAUZMANN, Rev. Mod. Phys., **14**, 12 (1942).
14) F. KOLLMANN, Technologie des Holzes und Holzwerkstoffe, Bd. 1, Springer-Verlag, (1951).
15) W. TRAPP und L. PUNGS, Holzforsch., **10**, 65 (1956).
16) S. OKAMOTO, Kōbunshi, **10**, 516 (1961).
17) C. R. CALKINS, Tappi, **33**, 278 (1950).
18) Y. ISHIDA, M. YOSHINO and M. TAKAYANAGI, J. Appl. Polymer Sci., **1**, 227 (1959).
19) G. P. MIKHAILOV, A. I. ARTHYUKHOV and V. A. SHEVELEV, Polymer Sci. USSR., **11**, 628 (1969).
20) E. FUKADA, Wood Sci. Techn., **2**, 299 (1968).
21) R. G. ZHBANKOV, Polymer Sci. USSR., **8**, 1962 (1966).
22) C. P. SMITH, Dielectric Behavior and Structure, McGraw-Hill, New York-London, (1955).
23) A. SAWATARI, T. YAMADA and T. TAKASHIMA, Japan Tappi, **29**, 84 (1975).

24) Yu. V. ZELENEV and V. I. GLAZKOV, Polymer Sci. USSR., **14**, 17 (1972).
25) M. KIMURA, M. USUDA and T. KADOYA, Sen-i Gakkaishi, **30**, T221 (1974).
26) M. NORIMOTO and T. YAMADA, Wood Research, No. 54, 19 (1973).
27) H. W. VERSEPUT, Tappi, **34**, 573 (1951).
28) D. E. KANE, J. Polymer Sci., **18**, 405 (1955).
29) A. PANDE, Laboratory Practice, **18**, 1052,
30) A. VENKATESWARAN, J. Appl. Polymer Sci., **13**, 2469 (1969).
31) R. W. SILLARS, Proc. Phys. Soc., London, **A169**, 66 (1939).
32) T. NAKAJIMA and S. SAITO, J. Polymer Sci., **31**, 423 (1958).
33) S. SAITO and T. NAKAJIMA, J. Soc. Materials Sci., Japan, **8**, 315 (1959).
34) L. SEGAL, J. J. CREELY, A. E. MORTIN, Jr., and C. M. CONRAD, Tex. Res. J., **29**, 786 (1959).
35) P. H. HERMANS, J. J. HERMANS and D. VERMAAS, J. Polymer Sci., **1**, 169 (1946).
36) L. VALENTINE, J. Polymer Sci., **27**, 313 (1958).
37) M. NORIMOTO and T. YAMADA, Mokuzai Gakkaishi, **21**, 151 (1975).
38) A. CHARLESBY, J. Polymer Sci., **15**, 263 (1955).
39) F. A. BLOUIN and J. C. ARTHUR, Jr., Tex. Res. J., **28**, 198 (1958).
40) S. TAKAMUKU, Y. MIYAMOTO and Y. HACHIHAMA, Kogyo Kagaku Zasshi, **64**, 2027 (1961).
41) J. F. SALMAN and M. A. MILLETT, Ind. Eng. Chem., **44**, 2848 (1952).
42) N. G. MCCRUM, B. E. READ and G. WILLIAMS, Anelastic and Dielectric Effects in Polymeric Solids, John Wiley & Sons, Inc., (1967).
43) K. H. ILLERS, Makromol. Chem., **38**, 168 (1960).
44) G. P. MIKHAILOV, A. I. ARTYUKHOV and T. I. BORISOVA, Polymer Sci. USSR., **8**, 1383 (1966).
45) J. A. SAXTON, Proc. Roy. Soc., **A213**, 473 (1952).
46) P. H. HERMANS, Physics and Chemistry of Cellulose Fibers, Elsevier's Publ. Co., (1949).
47) M. NORIMOTO, H. NAKATSUBO and T. YAMADA, J. Soc. Materials Sci., Japan, **22**, 241 (1973).
48) A. VENKATESWARAN, Wood and Fiber, **6**, 46 (1974).
49) A. VENKATESWARAN, Wood Sci., **4**, 248 (1972).
50) H. SAIKI, Doctoral Dissertation, Kyoto Univ., (1968).
51) O. WIENER, Abh. Sach. Akad. d. Wiss. Math. Phys. Kl., **32**, 507 (1912).
52) K. YOSHIHARA, Butsuri Kogaku, Kyoritsu Shuppan, (1966).
53) M. NORIMOTO, T. TANAKA and T. YAMADA, Mokuzai Gakkaishi, **21**, 342 (1975).
54) T. TANAKA, M. NORIMOTO and T. YAMADA, J. Soc. Materials Sci., Japan, **24**, 867 (1975).
55) D. A. G. BRUGGEMAN, Ann. Physik, **24**, 636 (1935).
56) R. MARK, Cell Wall Mechanics of Tracheid, Yale Univ. Press, New Haven, (1967).
57) F. ONAKA and H. HARADA, J. Japan Forestry Soc., **33**, 60 (1951).
58) H. SAIKI, Memoirs College Agriculture, Kyoto Univ., No. 96, 47 (1970).
59) C. P. SMITH and C. S. HITCHCOCK, J. Am. Chem. Soc., **54**, 4631 (1932).
65) M. SUZUKI, Bull. Gov't Forest Exp. Sta., No. 212, 89 (1968).